Supporting Information

Noncovalent hybrid of Pd(phen)(OAc)$_2$ and st-DNA for enantioselective hydroamination of β-nitrostyrene with methoxyamine

Supporting Information

Mrityunjoy Pal,[a] Dulal Musib,[a] Maynak Pal,[a] Gopal Rana,[b] Govinda Bag,[a] Subrata Dutta,[c] and Mithun Roy*[a]

[a] Department of Chemistry, National Institute of Technology Manipur, Langol 795004, Imphal, Manipur (INDIA)

[b] Department of Chemistry, Jadavpur University, Kolkata 700 032, West Bengal, India.

[c] Department of Chemistry, Vellore Institute of Technology, Vellore -632014, Tamil Nadu (INDIA

E-mail: mithunroy@nitmanipur.ac.in, mithunroy.iisc@gmail.com

Supporting Information

Table of Content

1. General Consideration:

All reagents and solvents were purchased from Sigma Aldrich, SRL Co., TCI Co., and dried and purified before use by the usual procedures. For column chromatography, silica gel (60–120 mesh or 100–200 mesh) obtained from Sigma Aldrich Co. was used. A gradient elution using hexane and ethyl acetate was performed, based on Merck aluminium TLC sheets. ^{1}H NMR and ^{13}C NMR spectra were measured on a Bruker Avance DRX 400 spectrometer or JEOL JNM-AL 400 spectrometer using Me_4Si as an internal standard. Samples were dissolved either in $CDCl_3$ or $(CD_3)_2SO$. GC-MS analysis were performed in PerkinElmer Clarus 690 MS. Q-TOF ESI Mass spectra (MS) were recorded in Bruker Esquire 3000 Plus spectrophotometer (Bruker-Franzen Analytic GmbH Bremen, Germany). High-performance liquid chromatography (HPLC) analyses were performed with a Thermo fisher ultimate 3000 using an optically active Chiralcel OD-H chiral column and Daicel normal phase C18 column while the peak areas were obtained with Chromeleon software.

DNA binding using viscometer

The viscosity measurements were done using a Schott Gerate AVS 310 automated viscometer attached to a constant temperature bath at 37 °C. The concentration of ST DNA stock solution was 130 µM in a 5 mM Tris-HCl buffer. The palladium complex was added gradually in increasing concentration from 0 to 120 µM, and the viscosity was measured for each addition. The flow times were monitored with an automated timer. The data were presented by plotting the relative specific viscosity of DNA, $(\eta/\eta_0)1/3$ vs [complex]/[DNA], where η is the viscosity of DNA in the presence of complex and η_0 is the viscosity of DNA alone in 5 mM Tris buffer medium. The viscosity values were calculated from the observed flow time of CT DNA containing solutions (t), duly corrected for that of the buffer alone (t0), η) (t - t0).

2. Experimental details

2.1. Preparation of [Pd(phen)(O₂CCH₃)₂] complex

To a stirred solution of Pd(OAc)$_2$ (0.22 mmol, 1 equivalence) in 5ml Dichloroethane, a solution of 1,10-phenanthroline (0.2 mmol, 0.9 equivalence) in 2 ml Dichloroethane was added and stirred for 30 minutes and then filtered off to collect the yellow coloured precipitate.(Yield 74%).^{1}H NMR (400 MHz, CDCl$_3$, ppm): δ 8.63 (d, J= 4.0 Hz, 2H), 8.57 (d, J= 4.0 Hz, 2H), 7.98 (s, 2H), 7.83 (q, J=4.0 Hz, 2H), 2.20 (s, 6H). ^{13}C NMR (100 MHz, CDCl$_3$, ppm): δ 171.87, 150.66, 146.86, 138.71, 129.84, 127.27, 125.35, 23.49. Q-TOF ESI MS in MeOH: m/z [M-OAc]$^+$ 344.9749.

2.2. General procedure for synthesis of β-nitrostyrene [1a]

To a 25 ml round bottom flask charged with a magnetic stirring-bar was added AgNO$_3$ (2.5 equiv.), TEMPO (0.2 equiv.), Styrene (1 equiv.) and oven-dried molecular sieves (4 Å, 150 mg). The olefin (if it was liquid) and solvent (DCE, 2 mL) were added by microliter syringe respectively in nitrogen condition. The tube was placed in a preheated oil bath at 70 ºC and the reaction mixture was stirred vigorously for 12h. Then the reaction mixture was cooled to room temperature. The reaction mixture was worked up by 10% Isopropyl alcohol in Dichloromethane (5 ml X 3 times) with water. Finally, the organic layer was concentrated and was purified by column chromatography using silica gel (100-200 mesh size) using hexane / ethyl acetate (99:1) as the eluent to afford yellow solid (Yield 94%). ^{1}H NMR (400 MHz, CDCl$_3$, ppm): δ 8.03-8.00 (d, J= 12.0 Hz, 1H), 7.97–7.33(m, 5H). ^{13}C NMR (100 MHz, CDCl$_3$, ppm): δ 139.21, 137.20, 132.28, 130.15, 129.51, 129.27. GC-MS in MeOH: m/z [MH$^+$] 149.1188.

2.3. 1-methoxy-4-(2-nitrovinyl) benzene [1b]

Synthesized according to the general procedure as discussed in section 2.2 and purified by flash chromatography (97:3; hexane: ethyl acetate) to afford a yellow solid (yield 89%).^{1}H NMR (400 MHz, CDCl$_3$, ppm): δ 7.98-7.96 (d, J= 8.0 Hz, 1H), 7.50-7.48 (d, J= 8.0 Hz, 2H), 6.96-6.93 (d, J= 12.0 Hz, 2H), 3.86 (s,3H). ^{13}C NMR (100 MHz, CDCl$_3$, ppm): δ 163.04, 139.16, 135.12, 131.28, 131.03, 122.63, 115.02, 55.65. GC-MS in MeOH: m/z [MH$^+$] 179.2189.

2.4. 1-methyl-3-(2-nitrovinyl) benzene [1c]

Synthesized according to the general procedure as discussed in section 2.2 and purified by flash chromatography (99:1; hexane: ethyl acetate) to afford a yellow oil (yield 92%). ^{1}H NMR (400 MHz, CDCl$_3$, ppm): δ 7.99-7.96 (d, J= 12.0 Hz, 1H), 7.59-7.56 (d, J= 12.0 Hz, 1H), 7.35-7.32 (m, 2H), 7.31-7.30 (d, J= 4.0 Hz, 1H), 2.39 (s,3H). ^{13}C NMR (100 MHz, CDCl$_3$, ppm): δ 139.41, 139.33, 137.03, 133.13, 130.08, 129.82, 129.37, 126.48, 21.39. GC-MS in MeOH: m/z [MH[+]] 163.2576.

2.5. 1-fluoro-4-(2-nitrovinyl) benzene [1d]

Synthesized according to the general procedure as discussed in section 2.2 and purified by flash chromatography (98:2; hexane: ethyl acetate) to afford a yellow solid (yield 90%). ^{1}H NMR (400 MHz, CDCl$_3$, ppm): δ 7.98-7.96 (d, J= 8.0 Hz, 1H), 7.57-7.52 (m, 2H), 7.16-7.09 (m, 2H). ^{13}C NMR (100 MHz, CDCl$_3$, ppm): δ 166.04, 137.96, 136.93, 131.44, 131.37, 126.40, 116.97, 116.80. GC-MS in MeOH: m/z [MH[+]] 167.15351.39. GC-MS in MeOH: m/z [MH[+]] 163.2576.

2.6. 1-chloro-4-(2-nitrovinyl) benzene [1e]

Synthesized according to the general procedure as discussed in section 2.2 and purified by flash chromatography (99:1; hexane: ethyl acetate) to afford a yellow solid (yield 91%). ^{1}H NMR (400 MHz, CDCl$_3$, ppm): δ 7.97-7.94 (d, J= 12.0 Hz, 1H), 7.49-7.48 (d, J= 4.0 Hz, 2H), 7.43-7.42 (d, J= 4.0 Hz, 2H). ^{13}C NMR (100 MHz, CDCl$_3$, ppm): δ 138.44, 137.82, 137.50, 130.38, 129.87, 128.61. GC-MS in MeOH: m/z [MH[+]] 183.1884.

2.7. Asymmetric synthesis procedure of [3a-3b]

DNA catalyst solution was prepared by the same method as described by the G. Roelfes and co-workers. DNA based catalyst solution (20 mM Mops, pH 6.5) (1.3 mg/ml salmon testes DNA and 0.84 mM [Pd(phen)(O$_2$CCH$_3$)$_2$]) was obtained by mixing of a buffered solution of [Pd(phen)(O$_2$CCH$_3$)$_2$] (5 ml of a 2.5 mM) to a MOPS buffered solution of st-DNA (10 ml of a 2mg/ml solution in 30 mM Mops, prepared 24 hours in advance). β-nitrostyrene (0.3 mmol, 1 eq[v].) in 1,4-dioxane, methoxyamine hydrochloride (0.5 mmol, 1.5 eq[v].) and potassium carbonate (0.5 mmol, 1.5 eq[v].) were added to the DNA based catalyst buffer solution and stirred

at room temperature in an inert atmosphere for 24 hrs. After the full consumption of the starting material (monitored by TLC) the organic layer was extracted by 10% isopropanol in dichloromethane (5 ml X 3 times) and concentrated by rotary evaporator. The light yellow colour oil was collected by column chromatography by using hexane: ethyl acetate (95:5) (89 %). The optical purity was determined by HPLC on Chiralcel OD-H column [hexane/2-propanol = 90/10, flow rate = 1.0 mL/min, UV = 254 nm, 11.75 min (major), 17.35 min (minor)] to be 76% ee.

2.8 .O-methyl-N-(2-nitro-1-phenylethyl) hydroxylamine [2a]

^{1}H NMR (400 MHz, DMSO-d_6) δ ppm: 7.38-7.28 (m, 5H), 7.14-7.12 (d, J = 8.0 Hz, 1H), 4.90-4.86 (dd, J = 16.0 Hz, 1H), 4.82-4.78 (dd, J =16.0 Hz, 1H), 4.67-4.63 (m, 1H), 3.34 (s, 3H).^{13}C NMR (100 MHz, DMSO-d_6) δ ppm: 137.46, 128.93, 128.70, 128.42, 78.74, 62.50, 61.94. GC-MS in MeOH: m/z [MH$^+$] 196.0848. $[\alpha]_D^{25}$ = +15.3 (c 1.00, CH$_3$OH).

2.9. N-(1-(4-methoxyphenyl)-2-nitroethyl)-O-methylhydroxylamine [2b]

Following the general procedure of 3a, compound 3b was synthesized. ^{1}H NMR (400 MHz, DMSO-d_6) δ ppm = 7.28-7.27 (dd, J = 8.0 Hz, 2H), 7.02-7.01 (d, J = 4.0 Hz, 1H), 6.88-6.86 (dd, J = 8.0 Hz, 2H), 4.88-4.84 (dd, J=16.0, 1H), 4.76-4.72 (dd, J=16.0, 1H), 4.60-4.56 (m, 1H), 3.70 (s, 3H),3.33 (s, 3H). ^{13}C NMR (100 MHz, DMSO-d_6) δ ppm = 159.63, 129.63, 129.21, 114.29, 78.64, 61.99, 61.92, 55.62. GC-MS in MeOH: m/z [MNa$^+$] 249.0848.

2.10. O-methyl-N-(2-nitro-1-(m-tolyl) ethyl) hydroxylamine [2c]

Following the general procedure of 3a, compound 3c was synthesized. ^{1}H NMR (400 MHz, DMSO-d_6) δ ppm: 7.21-7.20(d, J= 4.0, 1H), 7.19-7.18(d, J= 4.0, 1H), 7.15-7.14 (d, J= 4.0, 1H), 7.10-7.08 (d, J=8.0, 2H), 4.87-4.83 (dd, J=16.0, 1H), 4.79-4.75 (dd, J= 16.0, 1H), 4.61-4.57(m, 1H), 3.34 (s, 3H), 2.26 (s, 3H). ^{13}C NMR (100 MHz, DMSO-d_6) δ ppm = 138.058, 137.35, 129.33, 128.99, 128.84, 125.42, 78.54, 62.52, 61.92, 21.52. GC-MS in MeOH: m/z [MH$^+$] 210.1004.

2.11. N-(1-(4-fluorophenyl)-2-nitroethyl)-O-methylhydroxylamine [2d]

Following the general procedure of 3a, compound 3d was synthesized. ^{1}H NMR (400 MHz, DMSO-d[6]) δ ppm: 7.43-7.41 (d, J = 8.0 Hz, 2H), 7.17-7.13 (dd, J=16.0, 2H), 7.12-7.11 (d, J= 4.0,1H), 4.90-4.85 (dd, J=20.0, 1H), 4.81-4.77 (dd, J=16.0, 1H), 4.68-4.64 (m, 1H), 3.33 (s, 3H). ^{13}C NMR (100 MHz, DMSO-d[6]) 161.43, 133.75, 130.58, 130.52, 115.78, 115.61, 78.26, 61.97, 61.65. GC-MS in MeOH: m/z [MH[+]] 214.0754.

2.12. N-(1-(4-chlorophenyl)-2-nitroethyl)-O-methylhydroxylamine [2e]

Following the general procedure of 3a, compound 3e was synthesized. ^{1}H NMR (400 MHz, DMSO-d[6]) δ ppm: 7.42-7.37 (m, 4H), 7.16-7.15(d, J= 4.0, 1H), 4.89-4.85 (dd J=16.0, 1H), 4.82-4.79(dd, J=12.0, 1H), 4.68-4.63 (m, 1H), 3.33 (s, 3H). ^{13}C NMR (100 MHz, DMSO-d[6]) 136.61, 133.28, 130.38, 128.87, 78.01, 62.00, 61.66. GC-MS in MeOH: m/z. [MH[+]] 230.0458.

3. DNA binding studies

DNA binding experiment was carried out in MOPS buffer (pH 6.5) using aqueous solutions of the complexes. The ratio of the absorbance of the DNA stock solution at 260 nm to that at 280 nm was found to be 1.92, which suggested the absence of proteins.[1-2] DNA concentration were determined by using an extinction coefficient of 12800 M^{-1}.cm^{-1} at 260 nm and expressed in terms of base molarity.[3] UV-vis absorption titration experiments were done using different concentrations of ST DNA keeping the metal complex concentration as constant at 30 mM. Due correction was made for the absorbance of the ST DNA itself. Samples were equilibrated with st-DNA for 2 min well before recording each spectrum. The equilibrium binding constant (K_b) was determined from a non-linear fitting of the plot of vs. [DNA] applying the McGhee-von Hippel (MvH) method and using the expression of Bard and co-workers:

$$\frac{[DNA]}{(\varepsilon_A - \varepsilon_f)} = \frac{[DNA]}{(\varepsilon_b - \varepsilon_f)} + \frac{1}{K_b(\varepsilon_b - \varepsilon_f)}$$

Where, K_b is the microscopic equilibrium binding constant for each site, [DNA] is the concentration of DNA in nucleotides, ε_f, ε_a and ε_b are the molar extinction coefficients of the free complex in solution, the complex bound to DNA at a definite concentration and the complex in completely bound form with ST DNA, respectively.[4-5] The nonlinear least-squares

analysis was done using Origin Lab, v. 6.0. The binding constant value of [Pd(phen) $(O_2CCH_3)_2$] complex was found to be 1.5×10^5 M^{-1}.

4. Computational Methods

All the calculations were carried out using DFT (Density Functional Theory) with the Gaussian 09 program package.[6] For geometry optimizations, the 6-31G(d,p) basis set was used for the C, N, O, H elements, and the LANL2DZ pseudo potential for Pd. On the basis of these optimized geometries, single-point calculations were carried out with the 6-311+G(2d,2p) basis set for all elements. The stationary points were confirmed as transition states by analytical frequency calculations at the same basis set level as the geometry optimizations. The reported energies are Gibbs free energies, which include zero-point vibrational corrections, thermal and entropy corrections at 298 K. The latter are calculated as single-point corrections on the optimized structures with the same basis set combination used for the geometry optimizations, using the conductor-like polarizable continuum model (CPCM) method. On the basis of the optimized geometries, all energies were also corrected with single-point dispersion effects using the DFT method. To elucidate the reaction mechanism of the palladium catalyst with β-nitrostyrene and their thermochemistry was investigated by DFT calculation using the conductor-like polarisable continuum model (CPCM) method. We firstly optimized all the reactant, transition state and product by DFT calculation. After getting more stable conformer from DFT, we calculate the frequency calculation to get Gibbs free energy for the particular state. The Gibbs free energy of all the reactant, transition state and product are given in table S1. The energy barriers of the transition state 1 and reactant is $\Delta G = $ ~53.37 kcal/mol, illustrating a formation of η^3 styrene complex. We were unable to isolate these complexes may be this state is very fast intramolecular processes. The energy barriers of transition state 1 and transition state 2 is $\Delta G = $ ~36.29 kcal/mol, which suggest that the formation of stable three-member ring with palladium complex. The energy barriers of transition state 2 and transition state 3 is $\Delta G = $ ~6.96 kcal/mol which suggest the possibility of palladium β-nitrostyrene converted to the product and palladium acetate via hydride transfer. Finally, it is promising to develop β-nitrostyrene to product in presence of palladium catalyst via hydride transfer.

Table S1: Gibb's Free Energy (Kcal/mol) of the intermediates or transition state in Pd-catalysed hydromination reaction of β-nitrostyrene

State	Gibbs free energy (Kcal/mol)
β-nitro styrene	63.04532
[Pd(phen)(OAc)$_2$]	94.020358
[Pd(phen)(OAc)(OH)]	88.07065
[Pd(phen)(β-nitro styrene)(OAc)] [**TS-1**]	204.443885
[Pd(phen)(β-nitro styrene)] [**TS-2**]	168.200813
[Pd(phen)(β-nitro styrene)(H)] [**TS-2**]	161.9185
O-methyl-N-(2-nitro-1-phenylethyl)hydroxylamine (product)	109.077609

5. Molecular Docking studies

In our current work DNA plays an important role as an asymmetric catalyst providing the chiral site by intercalating the Pd Complex and inducing the asymmetry in the product. There are two type of grooves present in DNA, major grove and minor groove. The interaction of binding mode can be non-covalent binding, covalent binding, long range assembly. The binding modes of the Transition states can be determined and their interaction energy gives us a brief idea about the mechanism. The structures of the complex and the transition states are optimized using Gaussian 09 software. The structure of specific DNA dodecamer 3'-TTACTGGCTCGGCCT-5' was modelled by Avogadro Software[7] and the molecular docking was performed using Autodock 4.2 software[8] and Biovia Discovery Studio 9 molecular graphics programme[9] was used for visualization of the docked pose.

Molecular Docking has immerged as a useful tool for studying the non covalent interactions between a macromolecule and the entering ligand. The optimized structures were obtained from Gaussian 09 software and they are converted into PDB format using Mercury software. The macromolecule DNA Dodecamer was imported into Autodock 4.2 and polar hydrogens are added and using Gasteiger partial charges added to the DNA macromolecule.[10] Grid maps of 60 X 70 X 120 Å grid points and 0.375 Å spacing is created by Autogrid.[11] Docking simulation is carried out in Autodock programme using Lamarckian genetic algorithm.[12] Initial position, orientation, and torsions of the ligand molecules were set indiscriminately. Dockings were carried out for 10 different runs which were set to close after a maximum of 250,000 energy conformations. The probable site of Hydride transfer is governed by the steric hindrance provided by the DNA as evident from the molecular surface of the DNA helix leading to the formation of the R isomer as the major isomer.[13-15]

6. Molecular Docking

Supporting Information

The forcefield was not restricted during the docking studies. The default forcefield parameter for autodock4 cannot recognise Pd metal. Hence the default force-field parameters for atom types are overrided using the "parameter_file" command in the GPF and DPF[1-2], using the string "atom_par Pd 1.34 0.048 12.000 -0.00110 0.0 0.0 0 -1 -1 4 # Non H-bonding".[16]

The docking studies were performed on DNA with grid centre at -14.665, 1.602, -3.646 (x,y,z coordinate) and grid size of 98 X 126 X 82 (x X y X z) with spacing 0.375 Å. The docking calculations were carried out by general algorithm parameters with 10 runs of population size 150. The maximum number of evaluations was set to be 25000000 (long) with the rate of gene mutation 0.02 and the rate of crossover mode 0.8. The other parameters were set to default and the output was set to Lamarckian GA format. The conformations with highest binding energy poses explained the mechanism.

Table S2: Molecular docking energies of the intermediates or transition state in Pd-catalysed hydroamination reaction of β-nitrostyrene

State	Binding Energy (Kcal/mol)	Inter molecular energy (Kcal/mol)	Van der Waals Hydrogen Bonding Desolvation Energy (Kcal/mol)	Electrostatic Energy (Kcal/mol)	Total internal energy (Kcal/mol)	torsional energy (Kcal/mol)	unbound energy (Kcal/mol)
2	-6.88	-7.78	-7.65	-0.12	-1.09	0.89	-1.09
TS-1	-6.29	-8.37	-8.11	-0.27	-1.79	2.09	-1.79
TS-2	-5.95	-6.85	-6.69	-0.16	-1.17	0.89	-1.17
TS-3	-6.09	-7.88	-8.23	0.35	-0.87	1.79	-0.87

References

1. V. G. Cohen, H. Eisenberg, *Biopolymers*, 1969, **8**, 45-55.
2. M. E. Reichmann, S. A. Rice, C. A. Thomas, P. Doty, *J. Am. Chem. Soc.,* 1954, **76**, 3047-3053.

3. R. P. Megens, G. Roelfes, *Chem. Commun.,* 2012, **48**, 6366-6368.
4. M. Roy, B. V. S. K. Chakravarthi, C. Jayabaskaran, A. A. Karande, A. R. Chakravarty, *Dalton Trans.,* 2011, **40**, 4855-4864.

5. M. T. Carter, M. Rodriguez, A. J. Bard, *J. Am. Chem. Soc.,* 1989, **111**, 24, 8901-8911.

6. Gaussian 09, Revision A.02, M. J. Frisch, G. W. Trucks, H. B. Schlegel, G. E. Scuseria, M. A. Robb, J. R. Cheeseman, G. Scalmani, V. Barone, G. A. Petersson, H. Nakatsuji, X. Li, M. Caricato, A. Marenich, J. Bloino, B. G. Janesko, R. Gomperts, B. Mennucci, H. P. Hratchian, J. V. Ortiz, A. F. Izmaylov, J. L. Sonnenberg, D. Williams-Young, F. Ding, F. Lipparini, F. Egidi, J. Goings, B. Peng, A. Petrone, T. Henderson, D. Ranasinghe, V. G. Zakrzewski, J. Gao, N. Rega, G. Zheng, W. Liang, M. Hada, M. Ehara, K. Toyota, R. Fukuda, J. Hasegawa, M. Ishida, T. Nakajima, Y. Honda, O. Kitao, H. Nakai, T. Vreven, K. Throssell, J. A. Montgomery, Jr., J. E. Peralta, F. Ogliaro, M. Bearpark, J. J. Heyd, E. Brothers, K. N. Kudin, V. N. Staroverov, T. Keith, R. Kobayashi, J. Normand, K. Raghavachari, A. Rendell, J. C. Burant, S. S. Iyengar, J. Tomasi, M. Cossi, J. M. Millam, M. Klene, C. Adamo, R. Cammi, J. W. Ochterski, R. L. Martin, K. Morokuma, O. Farkas, J. B. Foresman, and D. J. Fox, Gaussian, Inc., Wallingford CT, 2016.

7. M. D. Hanwell, D. E Curtis, D. C. Lonie, T. Vandermeersch, E. Zurek, G. R. Hutchison; "Avogadro: An advanced semantic chemical editor, visualization, and analysis platform" *Journal of Cheminformatics*, 2012, **4**,17.

8. G. M. Morris, R. Huey, W Lindstrom., M. F. Sanner, R. K. Belew, D. S. Goodsell, A. J.Olson, Autodock 4 and AutoDockTools 4: automated docking with selective receptor flexibility, *J. Computational Chemistry*, 2009, **16**, 2785-2791.

9. BIOVIA, D. S. (2015). Discovery studio modeling environment. San Diego, Dassault Systemes, *Release*, 4.

10. T.A. Halgren, *J. Comput. Chem*., 1998, **17**, 490-519.

11. G.M. Morris, D.S. Goodsell, *J. Comput. Chem*., 1998, **19**, 1639-1662.

12. F.J. Solis, R.J.B. Wets, *Research*, 1981, **6**, 1, 9-30.

13. N. M. E. Metwaly, M. G. El-Ghalban, *J. Mol. Liq.,* 2016, **220**, 265-276.

14. M.C. Zhu, X.Cui, S. Zhang, L. Liu, Z.B. Han, E. Gao, *J. Inorg. Biochem.,* 2016, **157**, 34-45.

15. D. Ajloo, M.E. Moghadam, K.Ghadimi, M. Ghadamgahi, A.A. Saboury, A. Divsalar, M. S.Mohammadi, K. Yousefi, *Inorganica Chim. Acta*, 2015, **430**, 144-160.

16. https://ccsb.scripps.edu/autodock/forcefields/#:~:text=The%20default%20force%2Dfi eld%20parameters,namely%20the%20filename%20of%20the%20%E2%80%9C.

2. E. Pahonțu, M. Proks, S. Shova, G. Lupașcu, D. C. Ilieș, Ș. F.

Bărbuceanu, L. I. Socea, M. Badea, V. Păunescu, D. Istrati, A. Gulea, D. Drăgănescu, C. E. D. Pîrvu, Applied Organometallic Chemistry, 33, 11 ,5185.
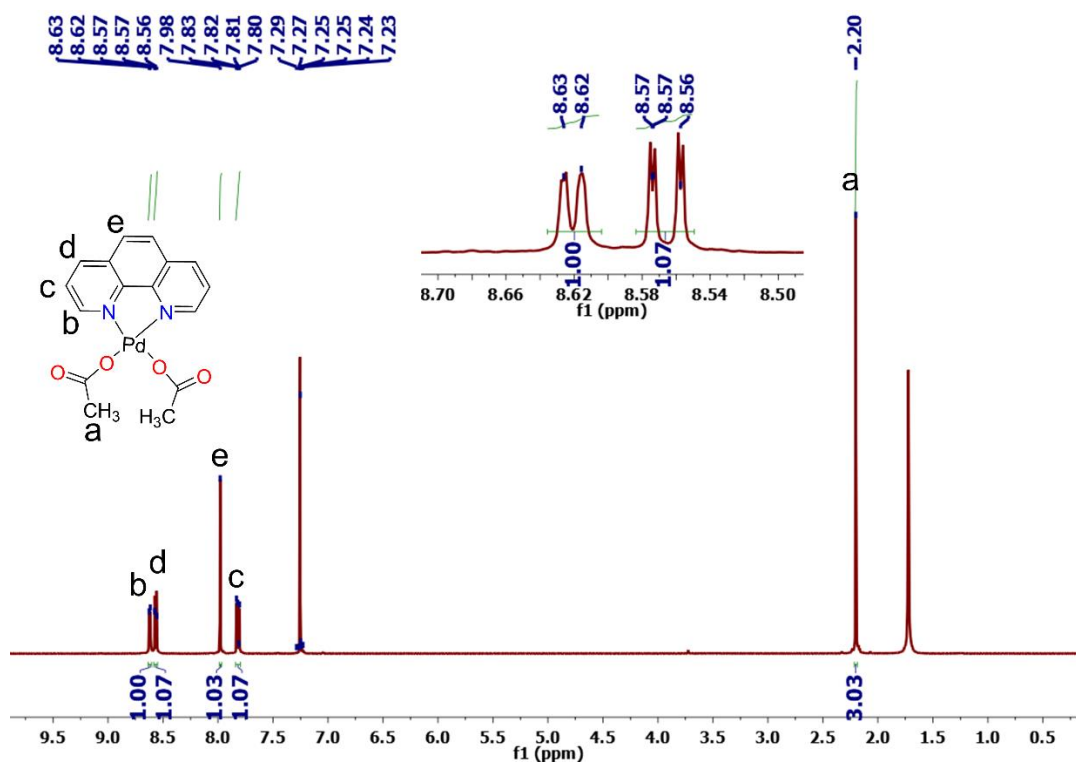

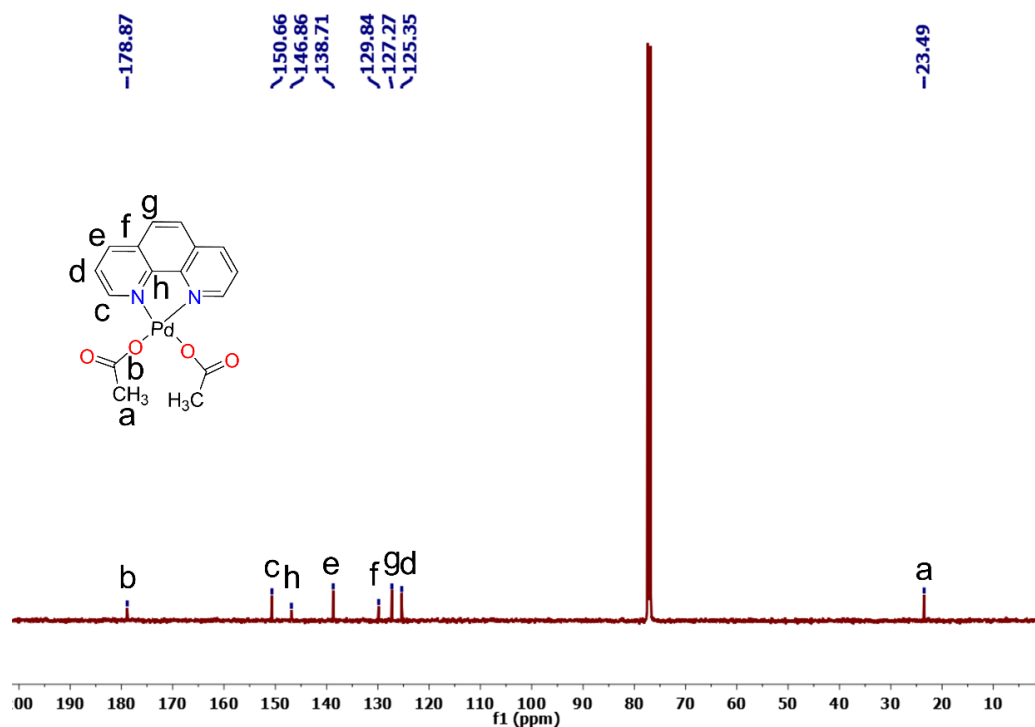**Figure S1:** ^{1}H NMR spectra of [Pd(phen)(O$_2$CCH$_3$)$_2$] complex in CDCl$_3$ using Bruker Avance DRX 400 (400 MHz) spectrometer.

Figure S2: ^{13}C NMR spectra of $[(phen)Pd(O_2CCH_3)_2]$ complex in $CDCl_3$ using Bruker Avance DRX 400 (100 MHz) spectrometer.
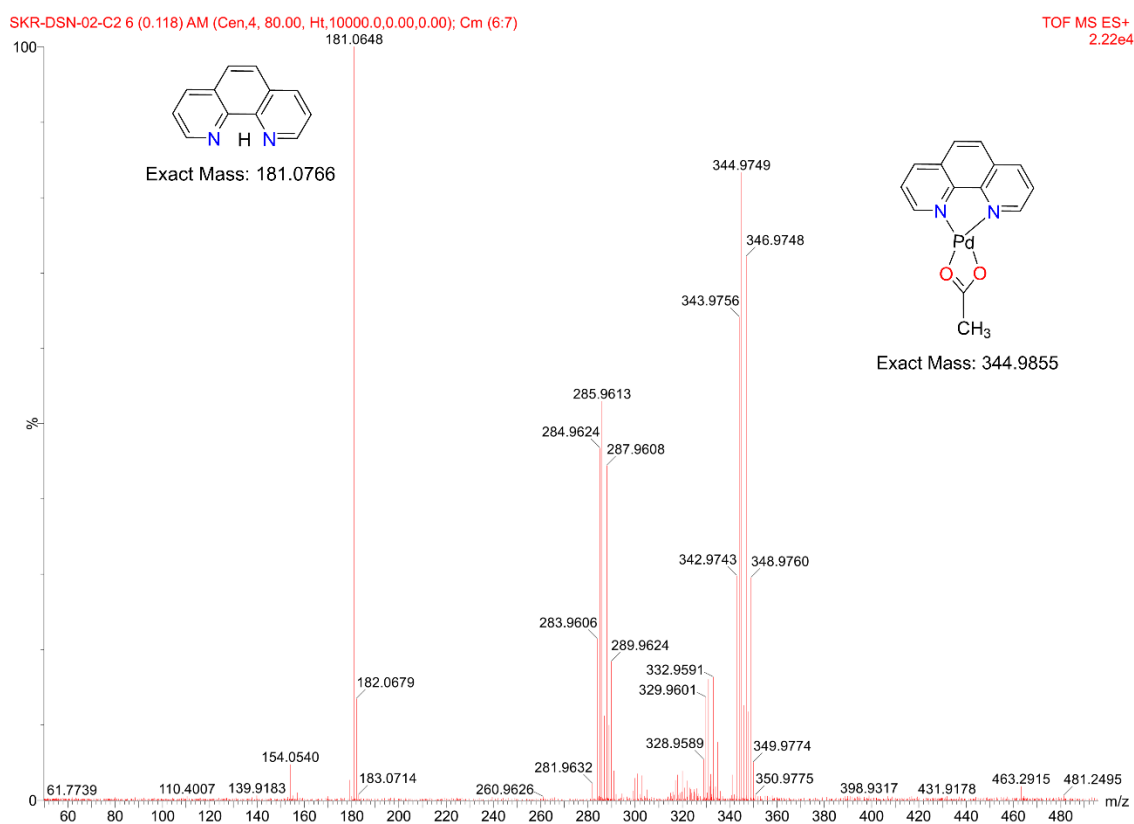

Figure S3: Q-TOF ESI-MS spectra of $[Pd(phen)(O_2CCH_3)_2]$ complex in CH_3OH.
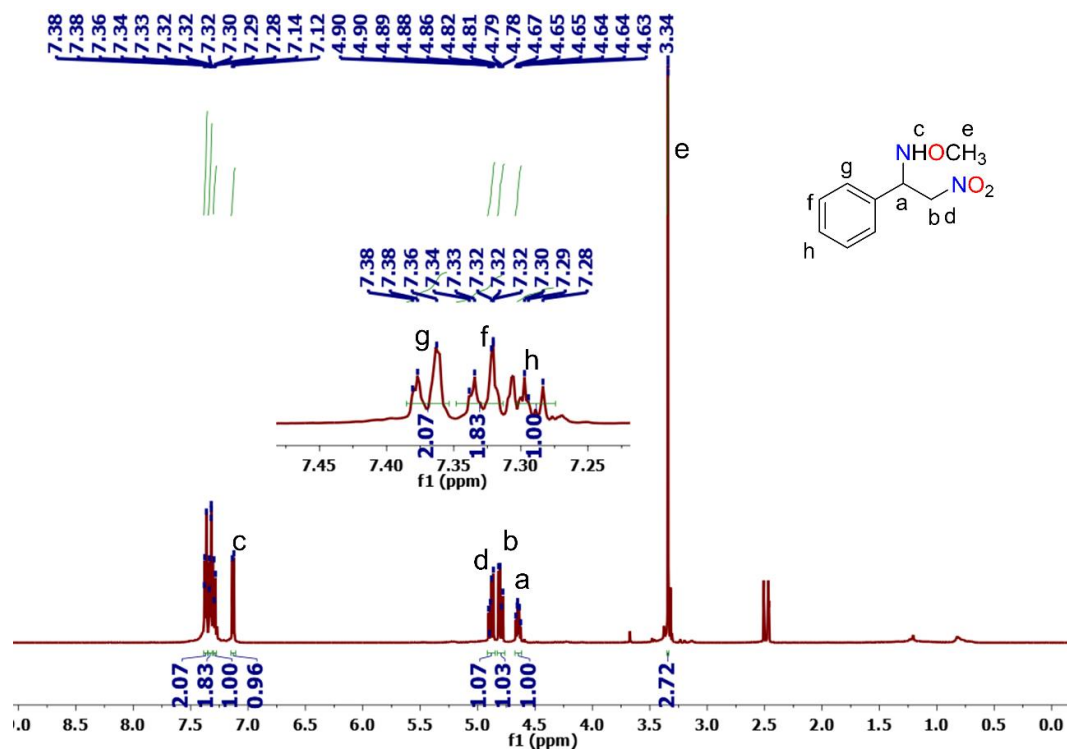
Figure S4: ^{1}H NMR spectra of O-methyl-N-(2-nitro-1-phenylethyl)hydroxylamine (2a) in DMSO-d_6 using Bruker Avance DRX 400 (400 MHz) spectrometer.
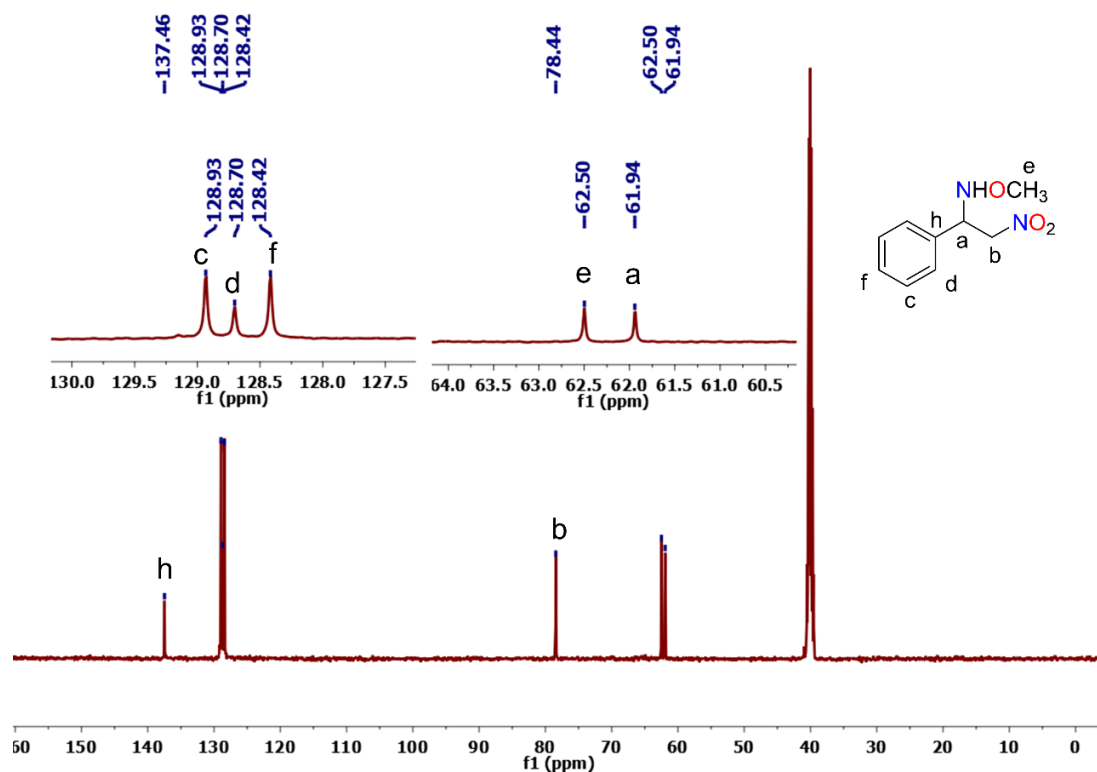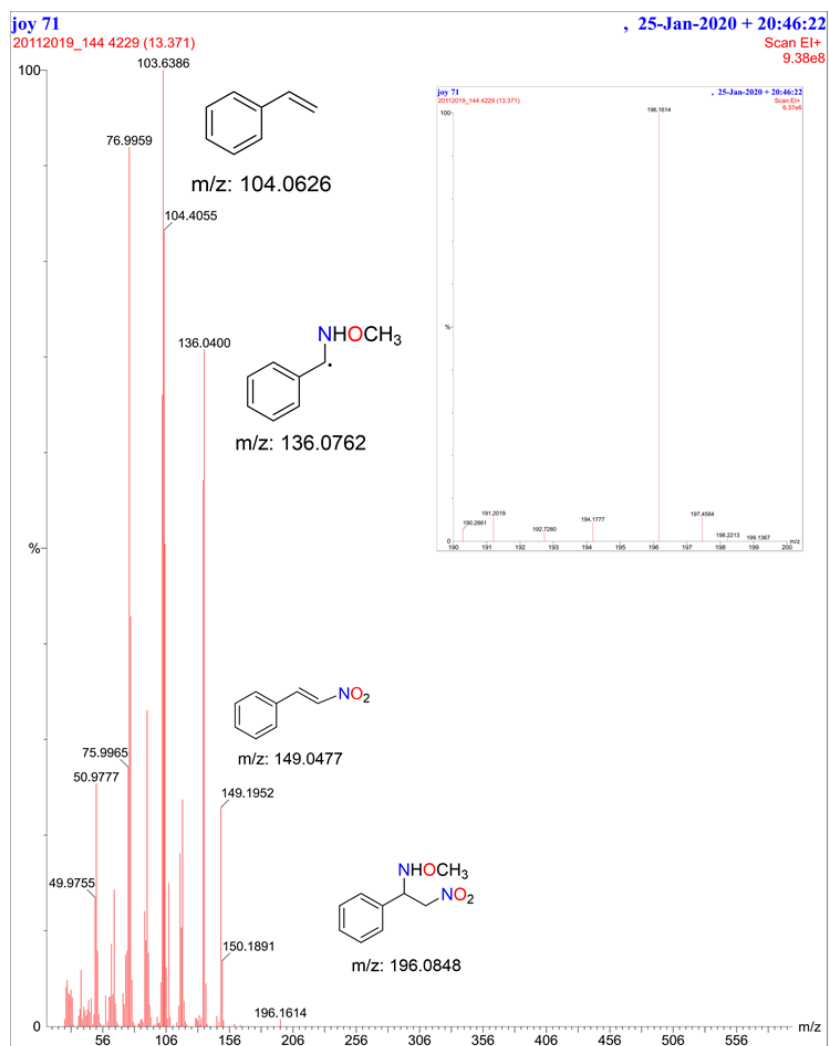

Figure S5: ^{13}C NMR spectra of O-methyl-N-(2-nitro-1-phenylethyl)hydroxylamine (2a) in DMSO-d_6 using Bruker Avance DRX 400 (100 MHz) spectrometer.

Figure S6: GC-MS spectra of O-methyl-N-(2-nitro-1-phenylethyl) hydroxylamine (2a) in CH3OH.
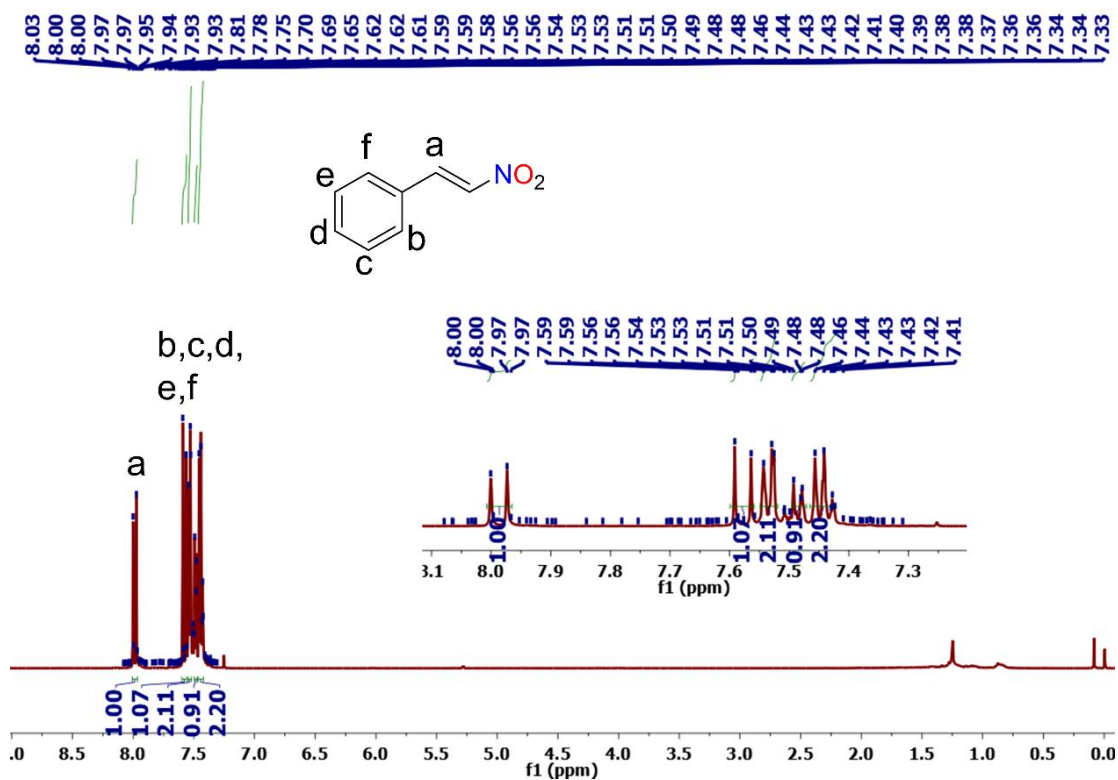
Figure S7: ^{1}H NMR spectra of β-nitrostyrene (1a) in CDCl$_3$ using Bruker Avance DRX 400 (400 MHz) spectrometer.
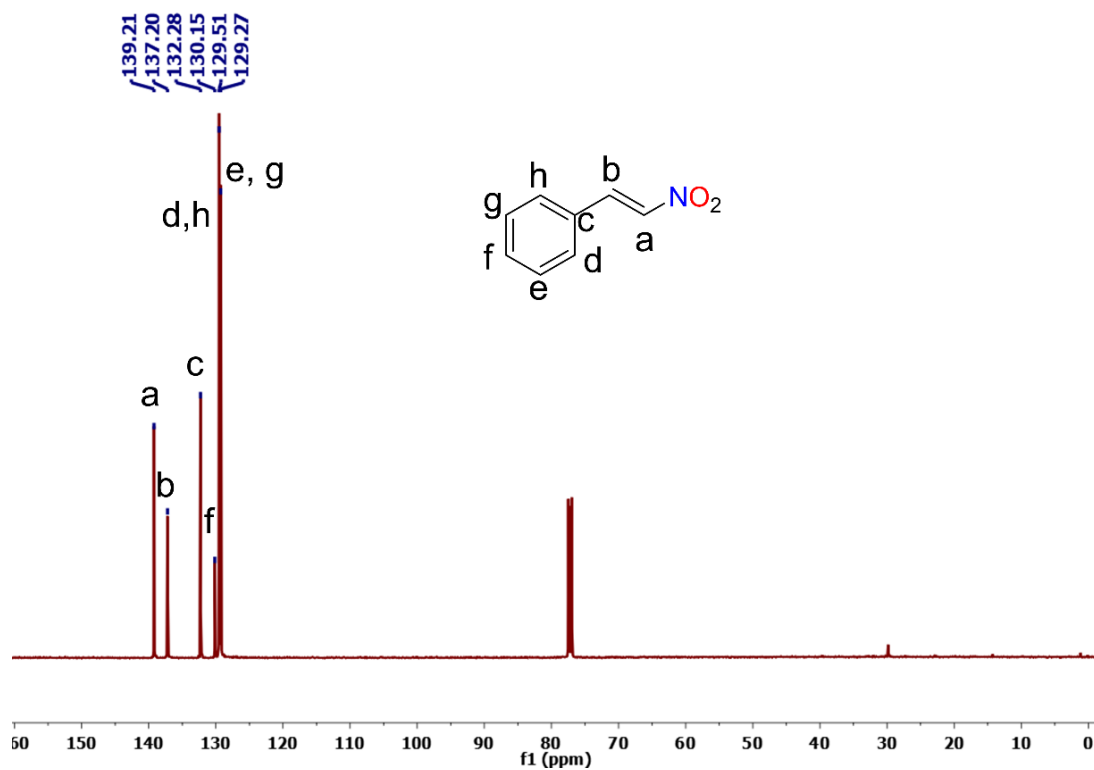
Figure S8: ^{13}C NMR spectra of β-nitrostyrene (1a) in CDCl$_3$ using Bruker Avance DRX 400 (100 MHz) spectrometer.
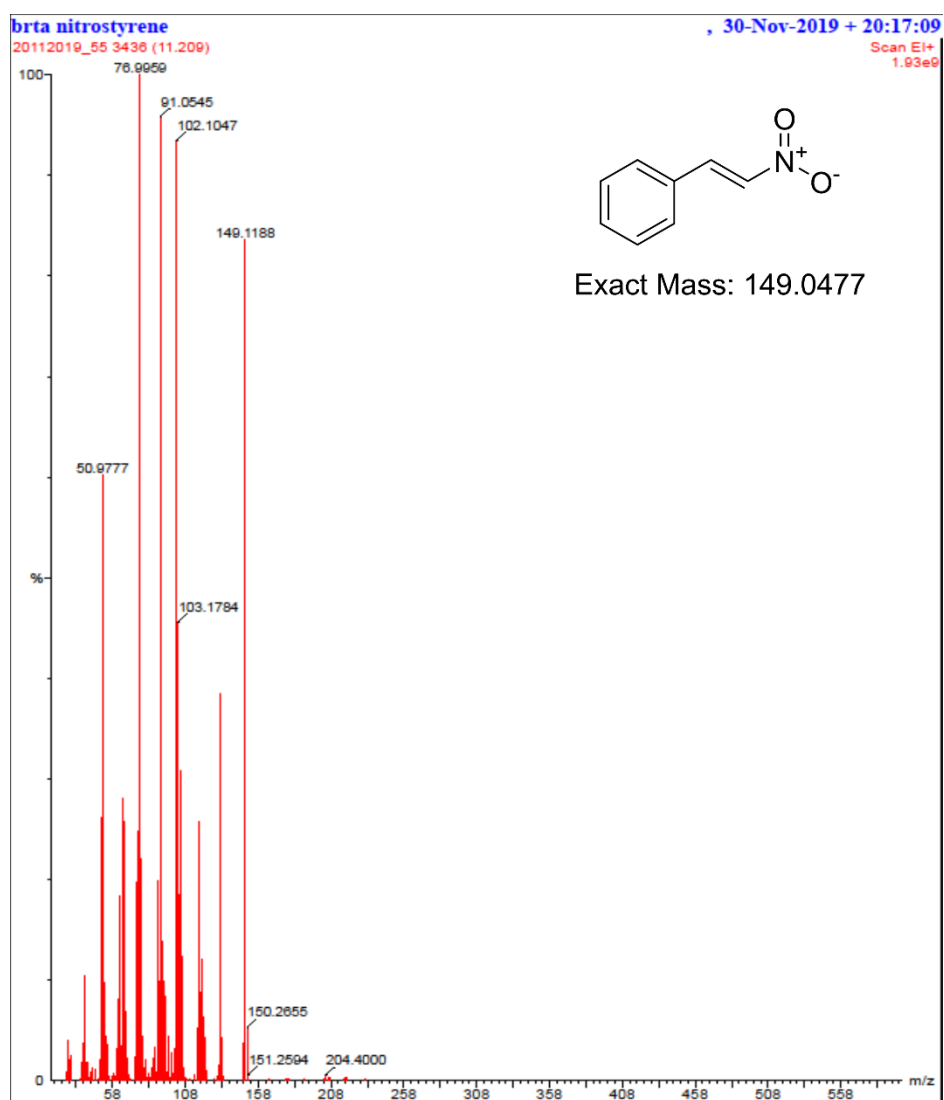
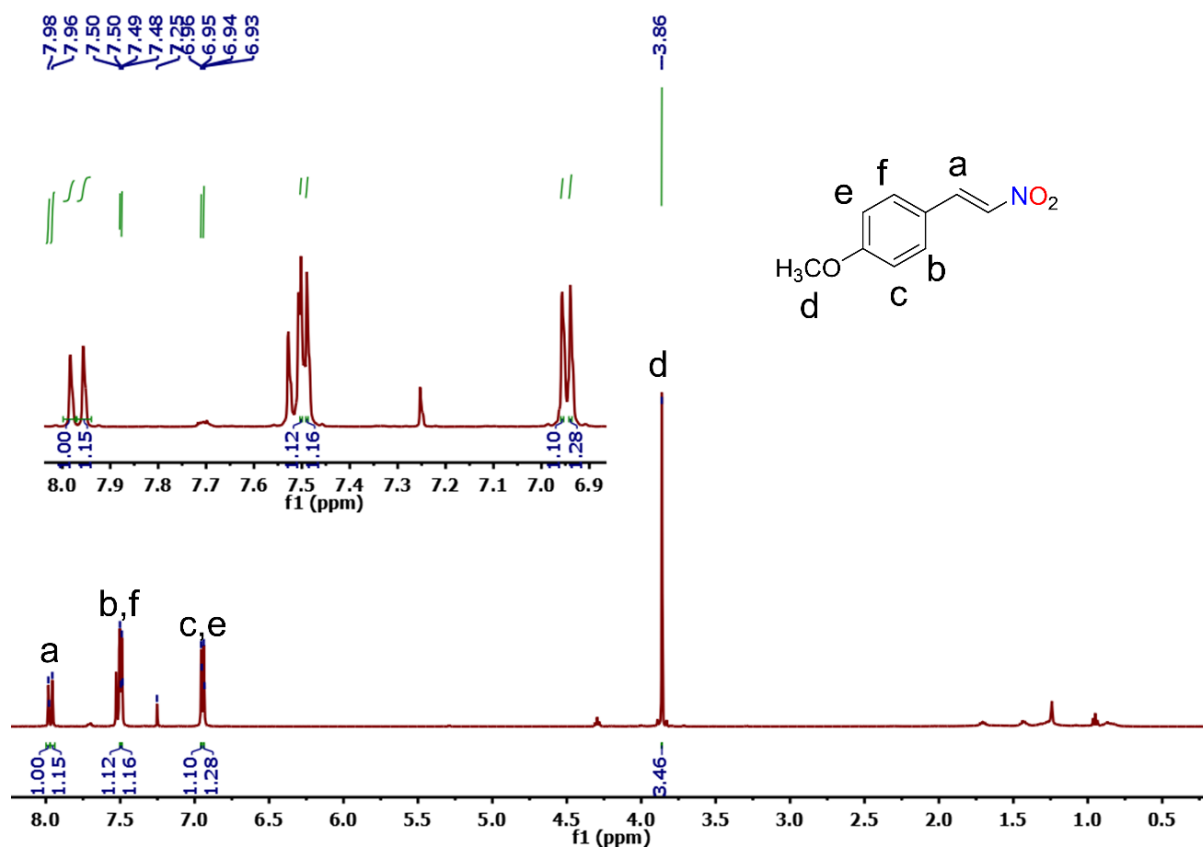**Figure S9**: GC-MS spectra of β-nitrostyrene (1a) in CH3OH.

Figure S10: ^{1}H NMR Spectra of 1-methoxy-4-(2-nitrovinyl) benzene (1b)in CDCl$_3$ using Bruker Avance DRX 400 (400 MHz) spectrometer.
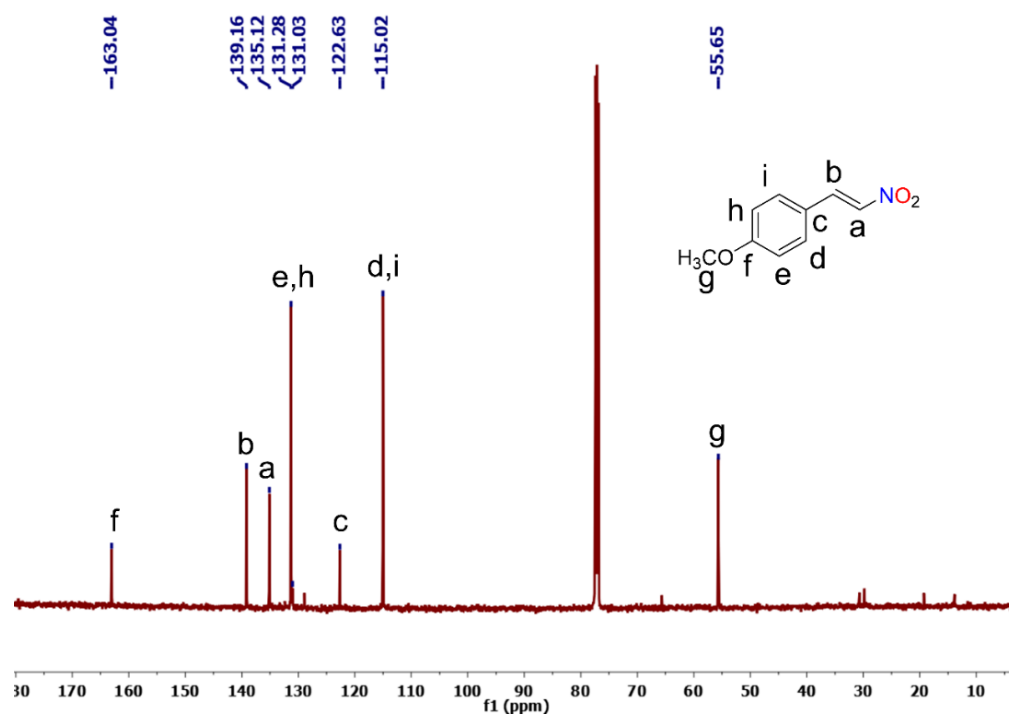
Figure S11: [^13]C NMR Spectra of 1-methoxy-4-(2-nitrovinyl) benzene (1b) in CDCl$_3$ using Bruker Avance DRX 400 (100 MHz) spectrometer.
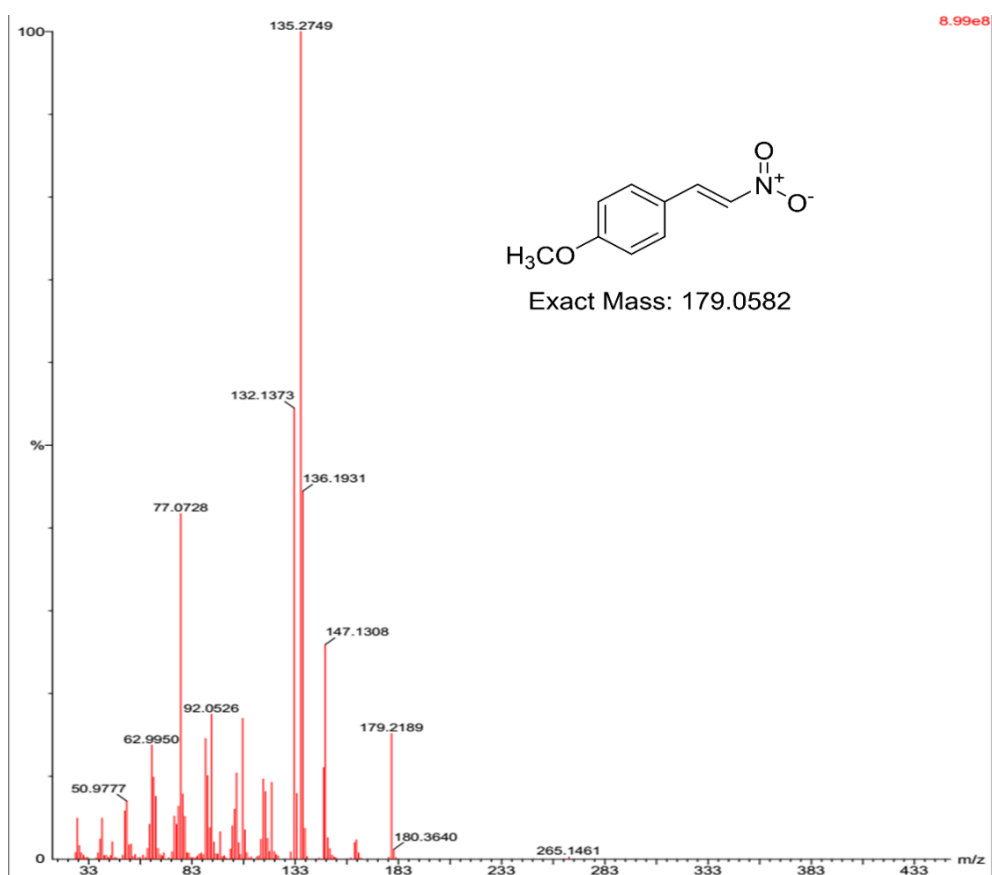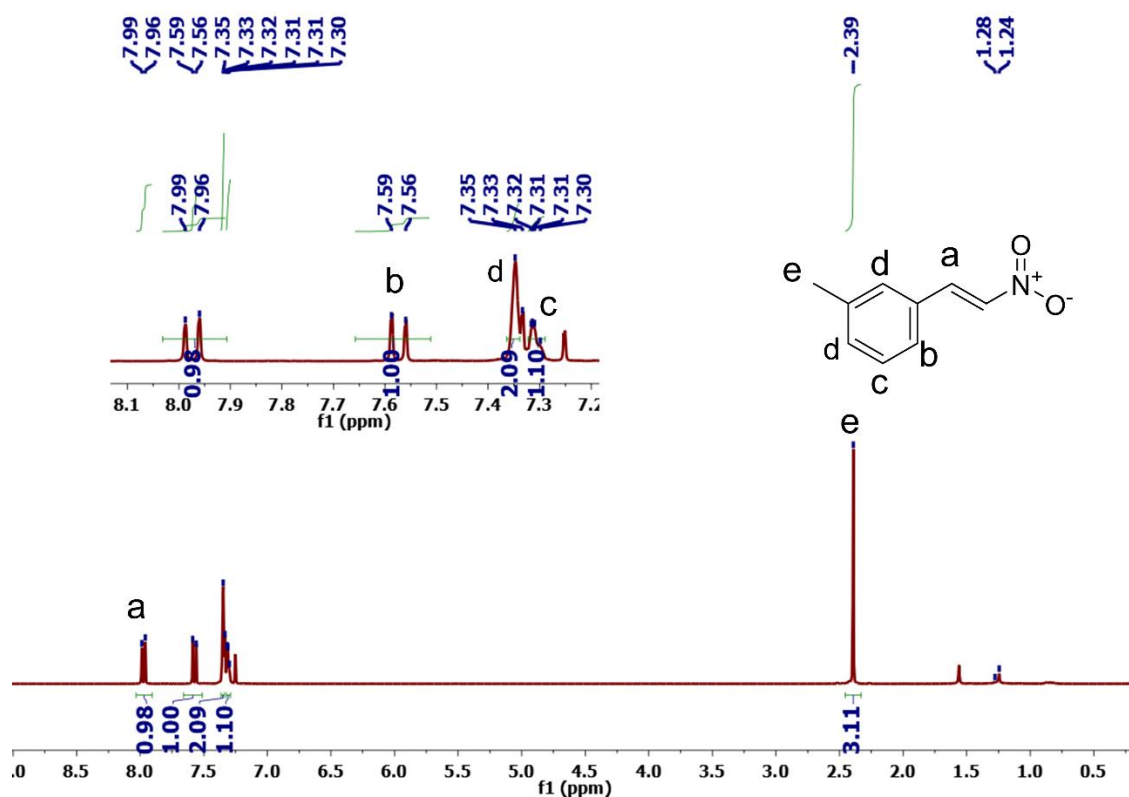
Figure S12: GC-MS Spectra of 1-methoxy-4-(2-nitrovinyl) benzene (1b) in CH$_3$OH.

Figure S13: ^{1}H NMR spectra of 1-methyl-3-(2-nitrovinyl) benzene (1c) in CDCl$_3$ using Bruker Avance DRX 400 (400 MHz) spectrometer.
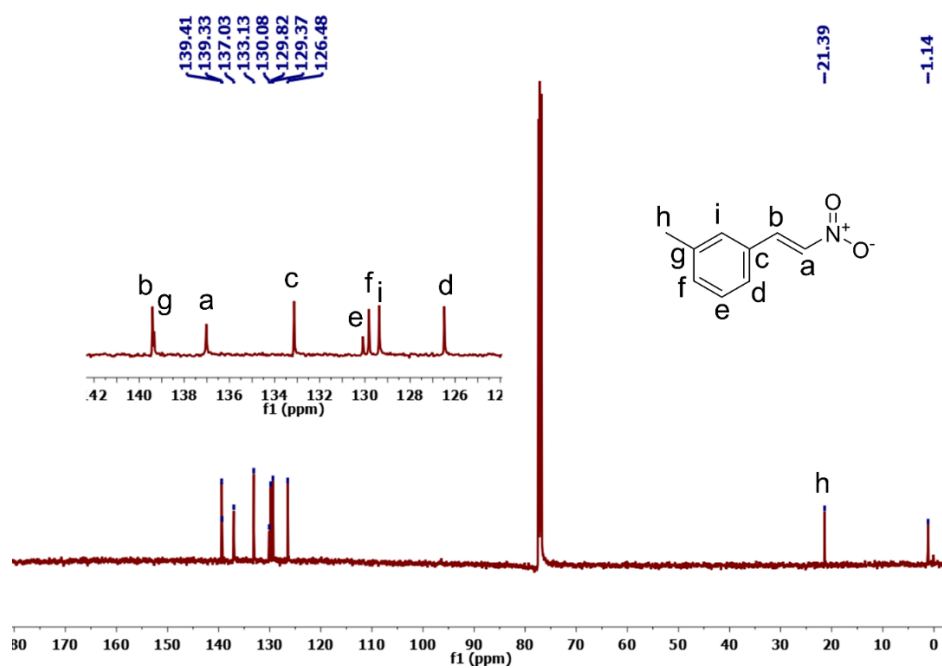
Figure S14: ^{13}C NMR spectra of 1-methyl-3-(2-nitrovinyl) benzene (1c) in CDCl$_3$ using Bruker Avance DRX 400 (100 MHz) spectrometer.
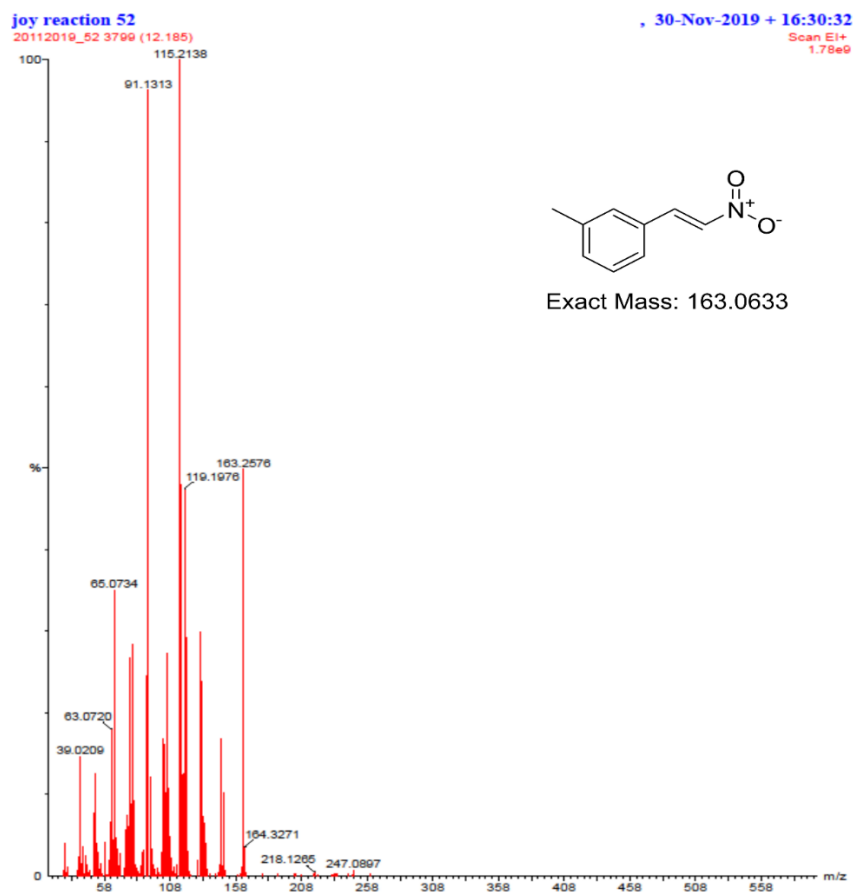

Figure S15: GC-MS spectra of 1-methyl-3-(2-nitrovinyl)benzene (1c) in CH$_3$OH.
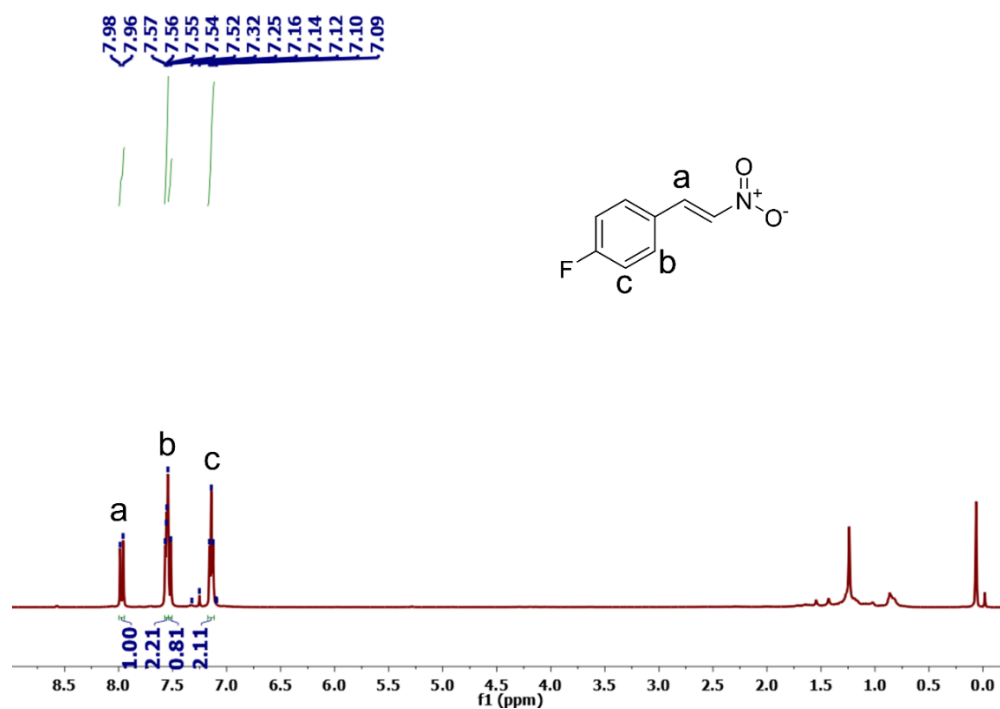
Figure S16: ^{1}H NMR spectra of 1-fluoro-4-(2-nitrovinyl) benzene (1d) in CDCl$_3$ using Bruker Avance DRX 400 (400 MHz) spectrometer.

Figure S17: ^{13}C NMR spectra of 1-fluoro-4-(2-nitrovinyl) benzene (1d) in CDCl$_3$ using Bruker Avance DRX 400 (100 MHz) spectrometer.

Figure S18: GC-MS spectra of 1-fluoro-4-(2-nitrovinyl) benzene (1d) in CH$_3$OH.

Figure S19:^{1}H NMR spectra of 1-chloro-4-(2-nitrovinyl) benzene (1e) in CDCl$_3$ using

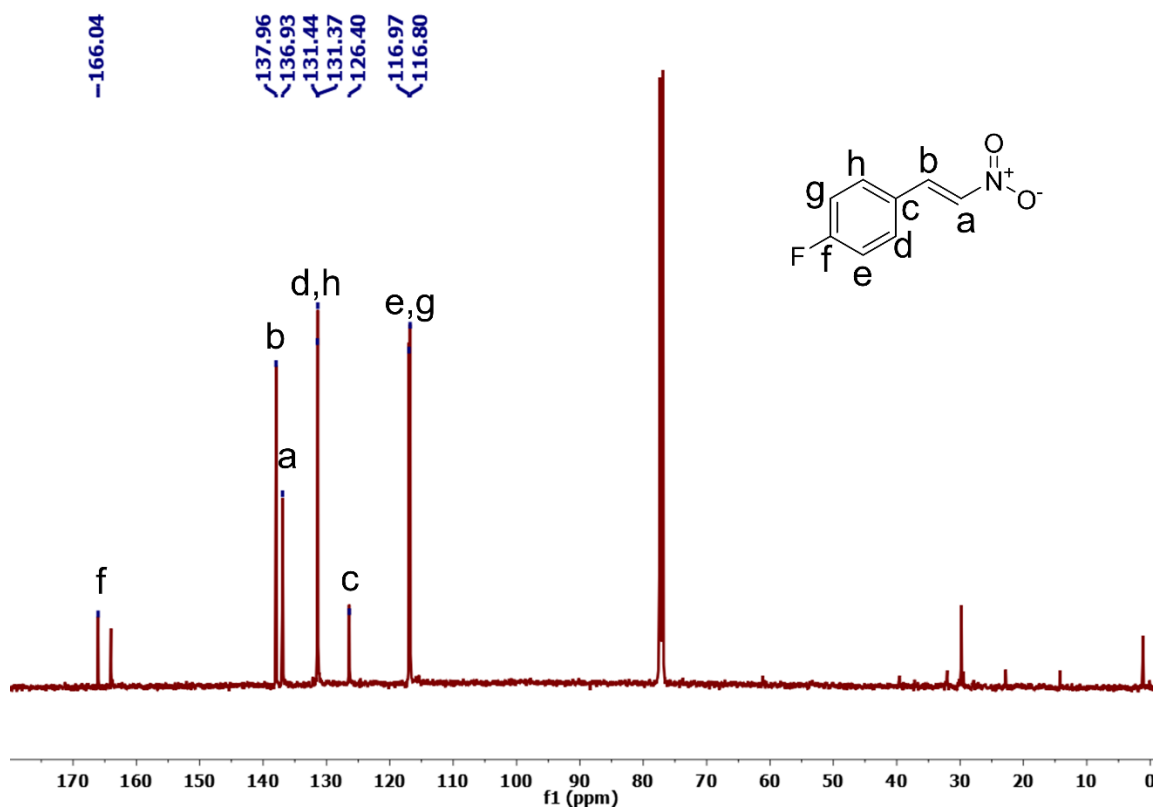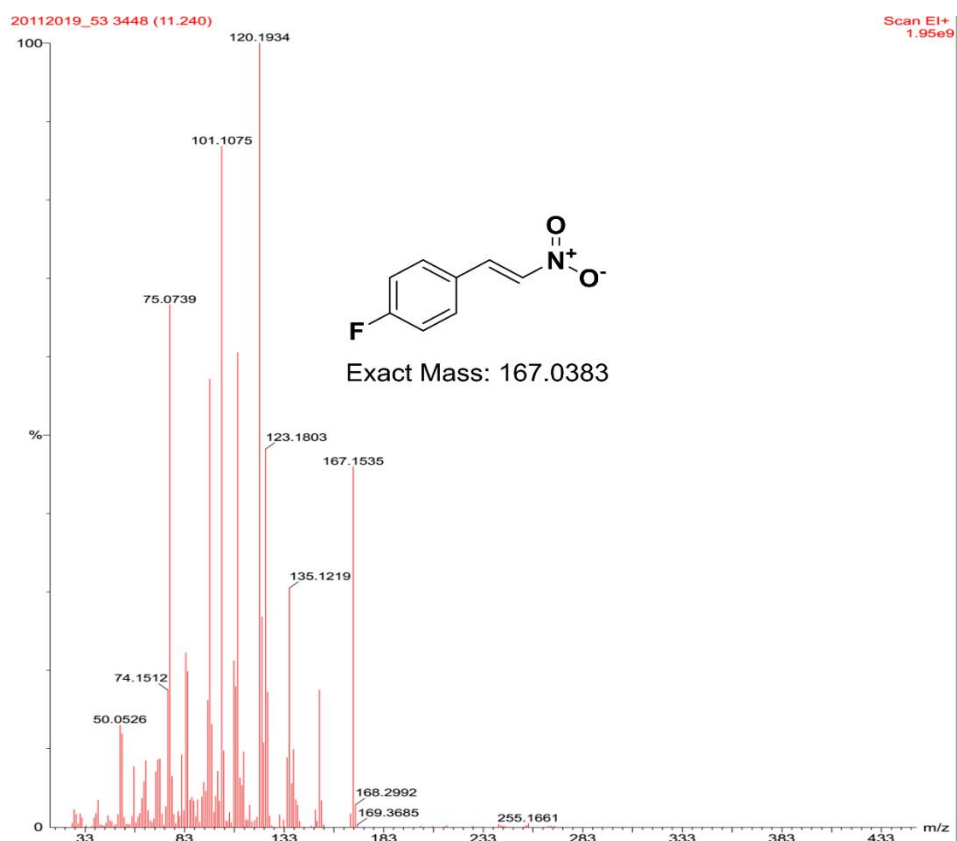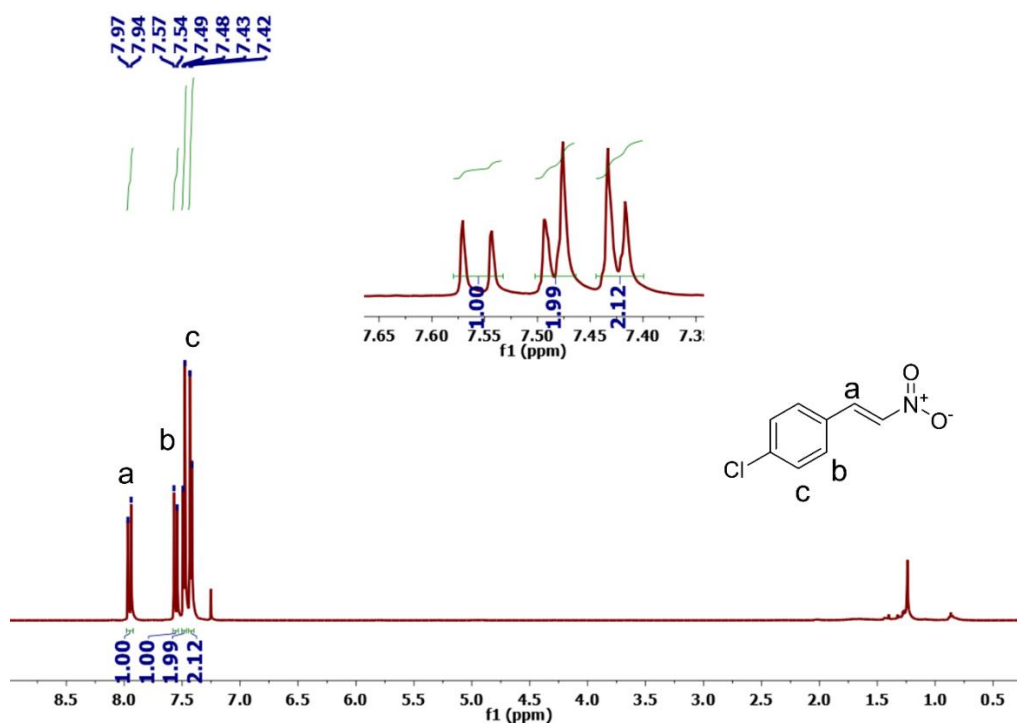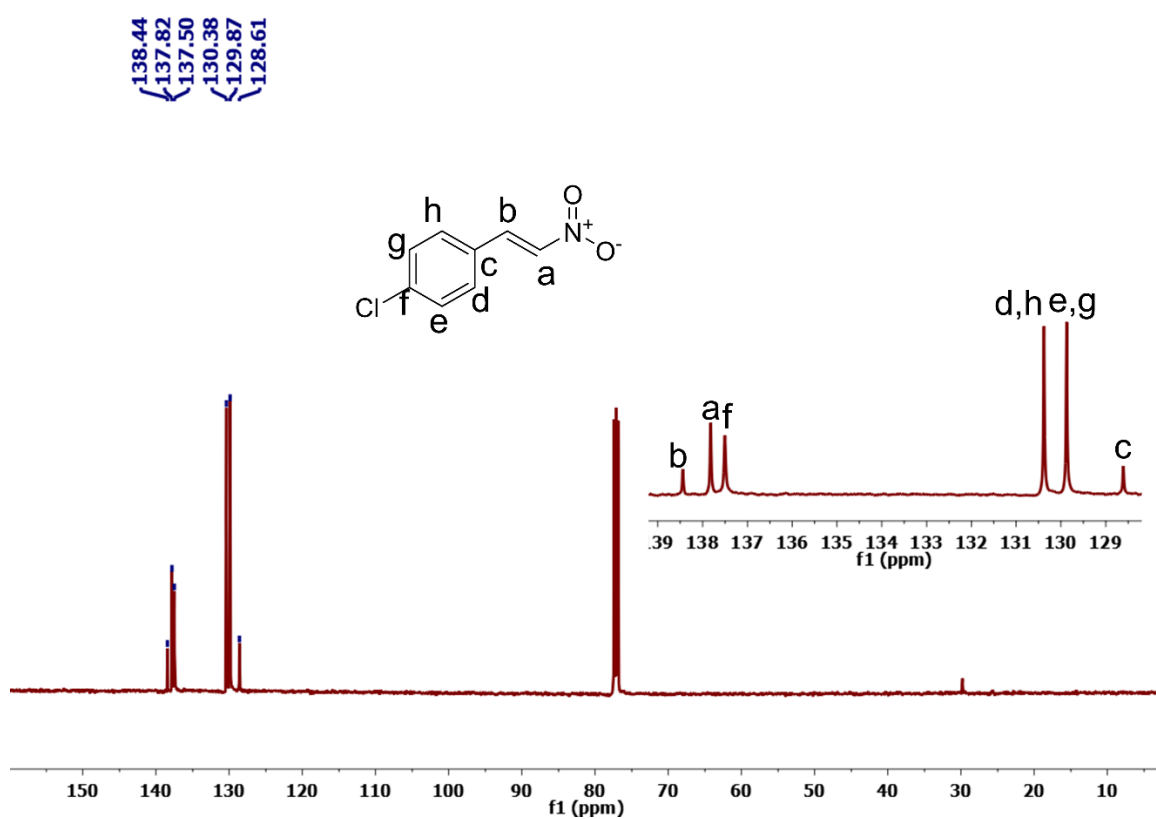Bruker Avance DRX 400 (400 MHz) spectrometer.

Figure S20: ^{13}C NMR spectra of 1-chloro-4-(2-nitrovinyl) benzene (1e) in CDCl$_3$ using Bruker Avance DRX 400 (100 MHz) spectrometer.

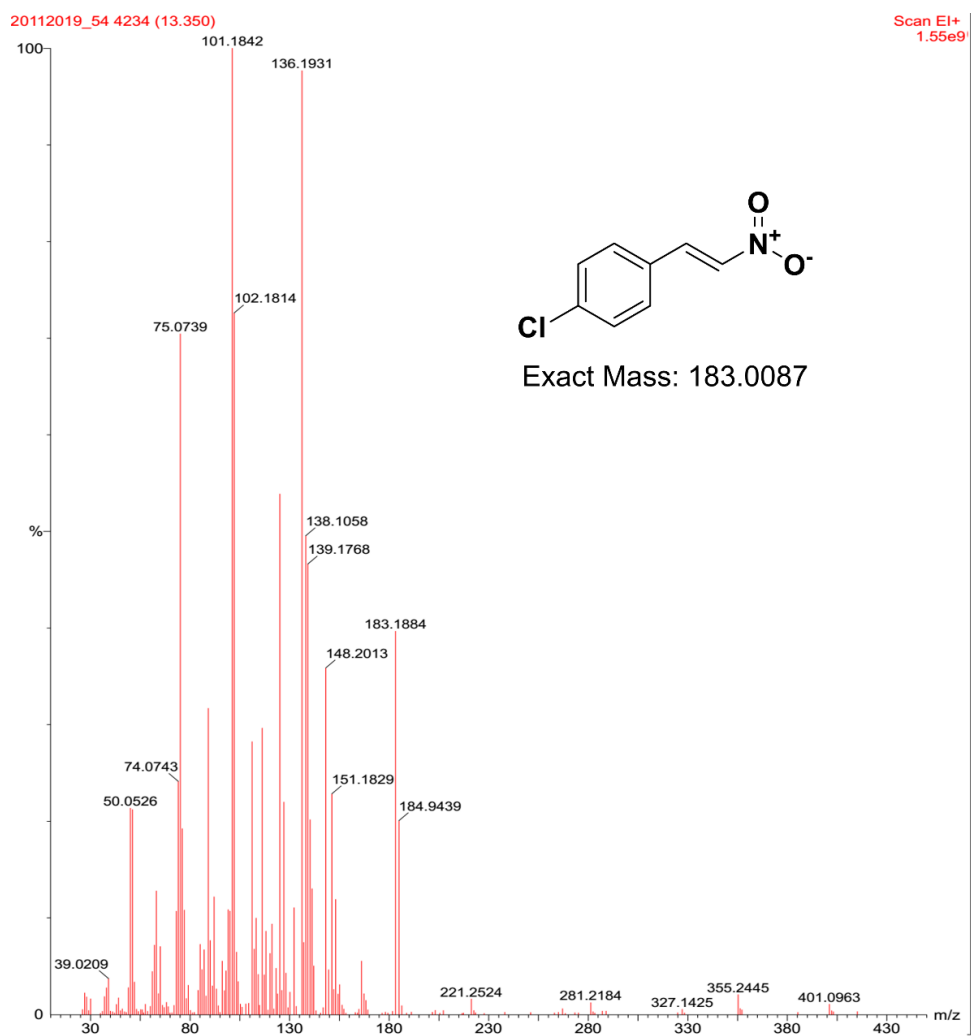**Figure S21**: GC-MS spectra of 1-chloro-4-(2-nitrovinyl) benzene (1e) in CH$_3$OH.

Figure S22: ^1H NMR spectra of N-(1-(4-methoxyphenyl)-2-nitroethyl)-O-methylhydroxylamine (2b) in DMSO-d_6 using Bruker Avance DRX 400 (400 MHz) spectrometer.

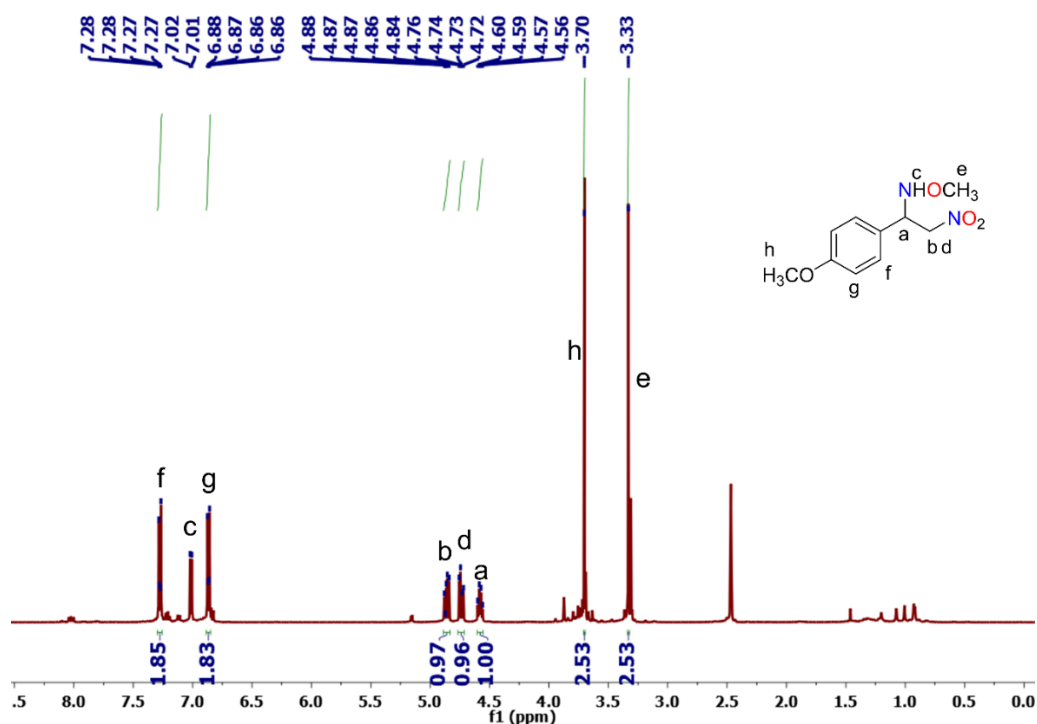**Figure S23:** ^{13}C NMR spectra of N-(1-(4-methoxyphenyl)-2-nitroethyl)-O-methylhydroxylamine (2b) in DMSO-d_6 using Bruker Avance DRX 400 (100 MHz) spectrometer.

20112019_433 7909 (23.211)

Scan EI+
3.82e7

207.2983

m/z: 135.0804

281.3708

m/z: 249.0848

209.1287

44.1143 73.2284

135.1219

191.3545

133.2853

96.3507

147.3602

267.2790

282.5894

249.2231

283.4272

325.2385

341.2314

357.0724 401.2487

475.3663

549.8235

m/z

Figure S24: GC-MS spectra of N-(1-(4-methoxyphenyl)-2-nitroethyl)-O-methylhydroxylamine (2b) in CH$_3$OH.

30

Figure S25: ^{1}H NMR spectra of O-methyl-N-(2-nitro-1-(m-tolyl) ethyl) hydroxylamine (2c) in DMSO-d_6 using Bruker Avance DRX 400 (400 MHz) spectrometer.

Figure S26: ^{13}C NMR spectra of O-methyl-N-(2-nitro-1-(m-tolyl) ethyl) hydroxylamine (2c) in DMSO-d_6 using Bruker Avance DRX 400 (100 MHz) spectrometer.
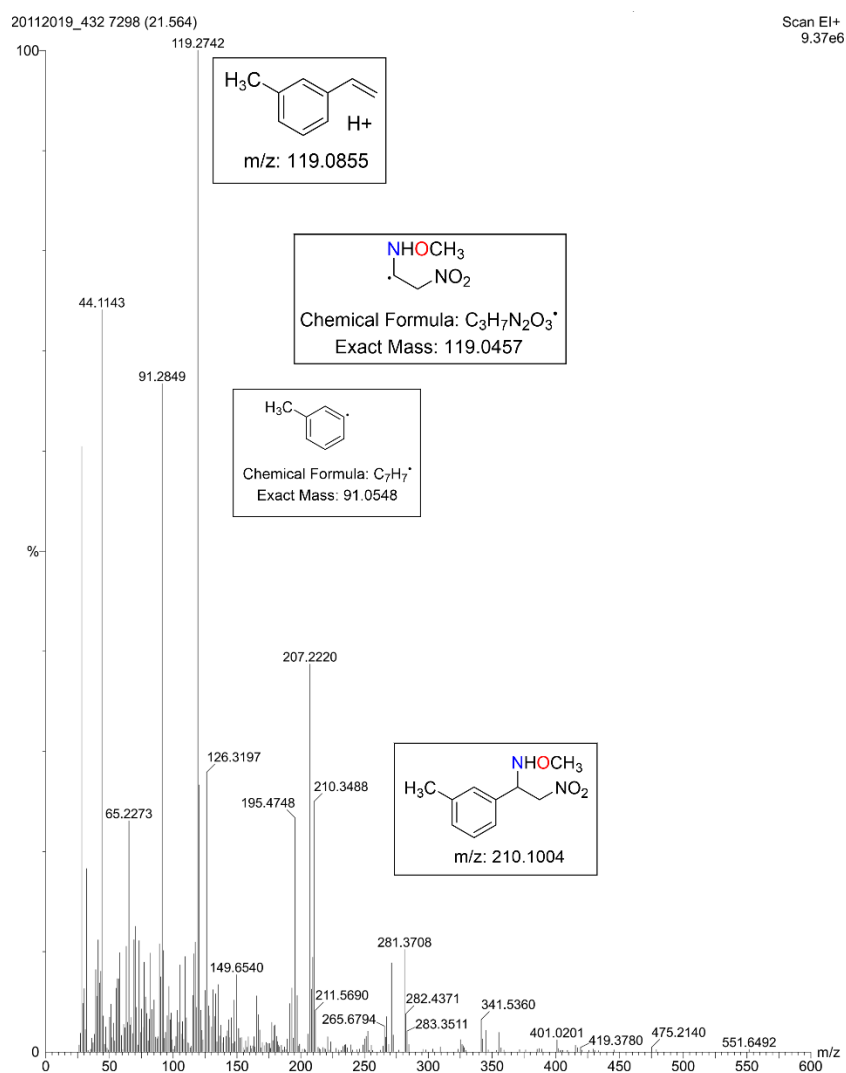
Figure S27: GC-MS spectra of O-methyl-N-(2-nitro-1-(m-tolyl) ethyl) hydroxylamine (2c) in CH$_3$OH.
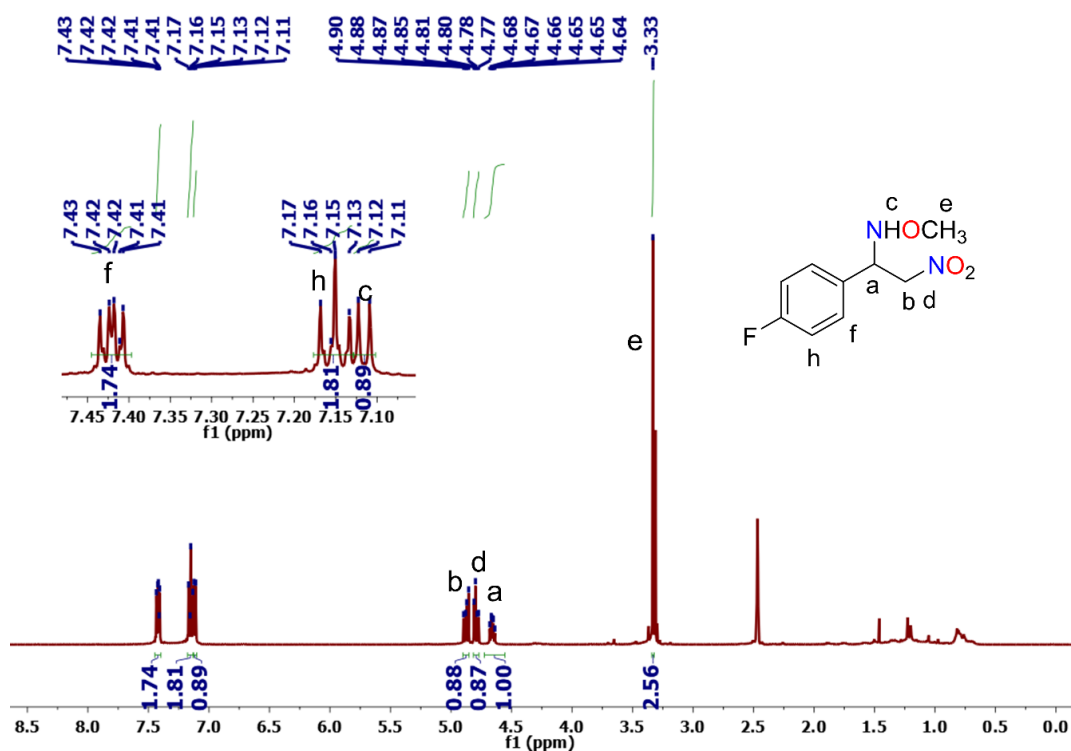
Figure S28: ^{1}H NMR spectra of N-(1-(4-fluorophenyl)-2-nitroethyl)-O-methylhydroxylamine (2d) in DMSO-d$_6$ using Bruker Avance DRX 400 (400 MHz) spectrometer.
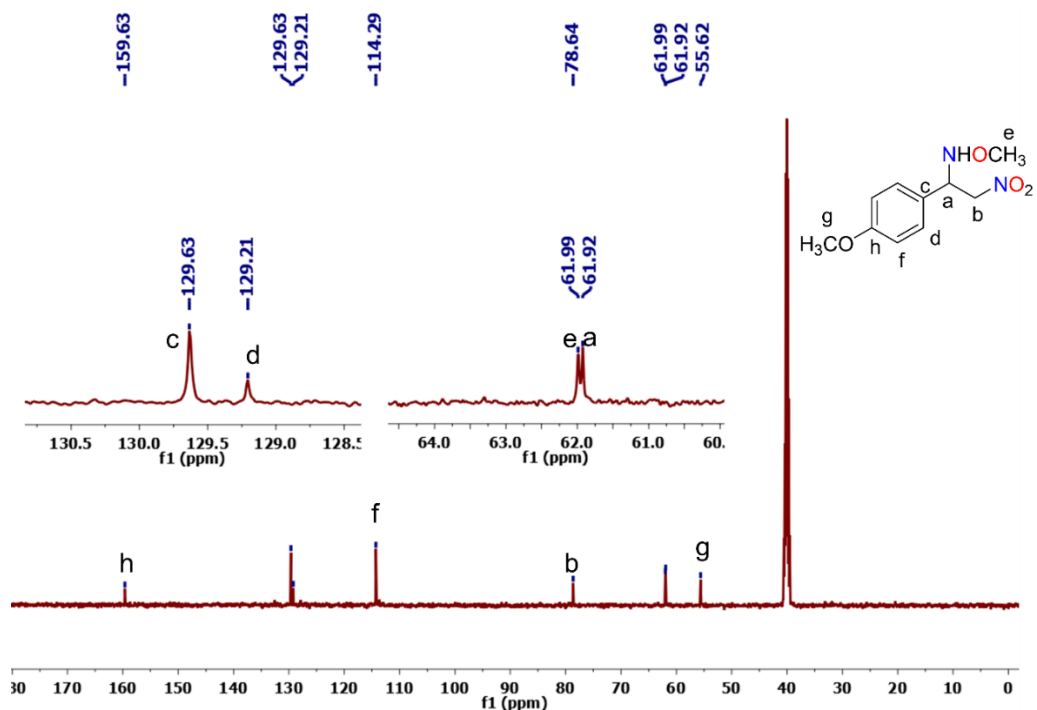

Figure S29: ^{13}C NMR spectra of N-(1-(4-fluorophenyl)-2-nitroethyl)-O-methylhydroxylamine (2d) in DMSO-d$_6$ using Bruker Avance DRX 400 (100 MHz) spectrometer.
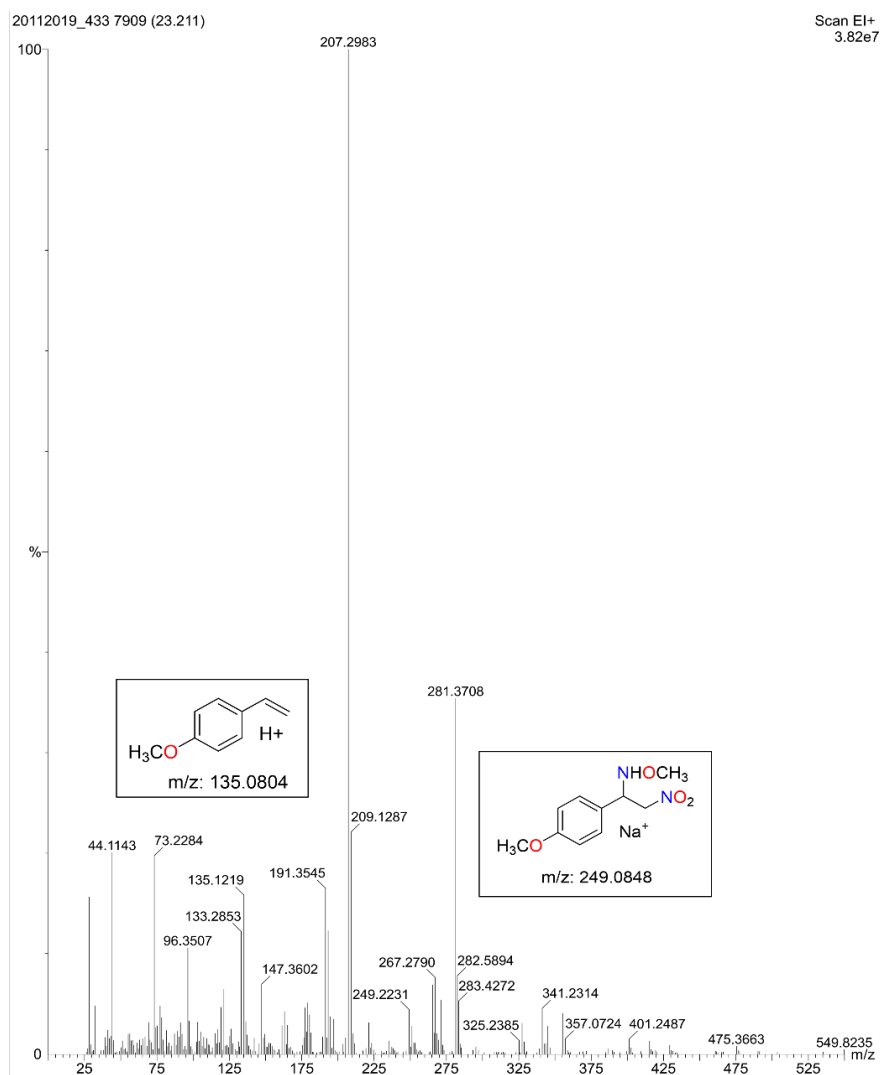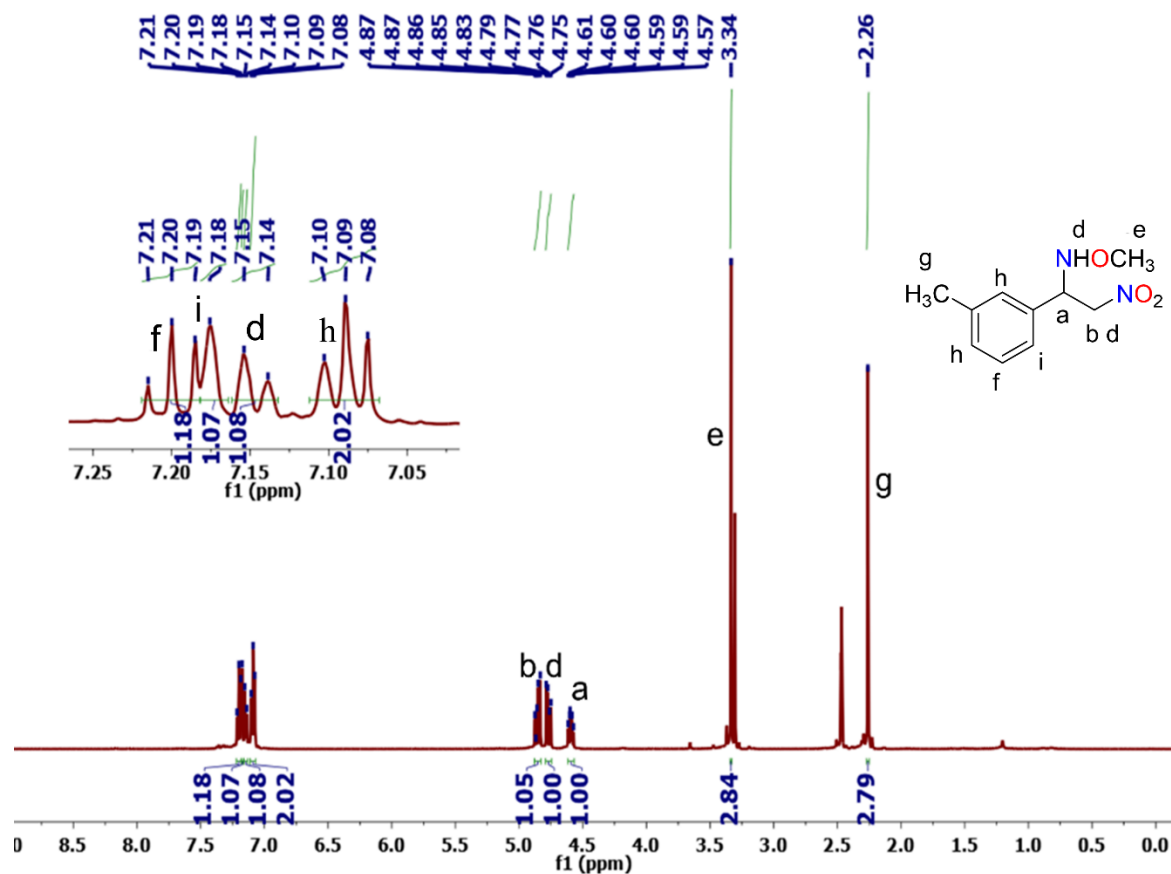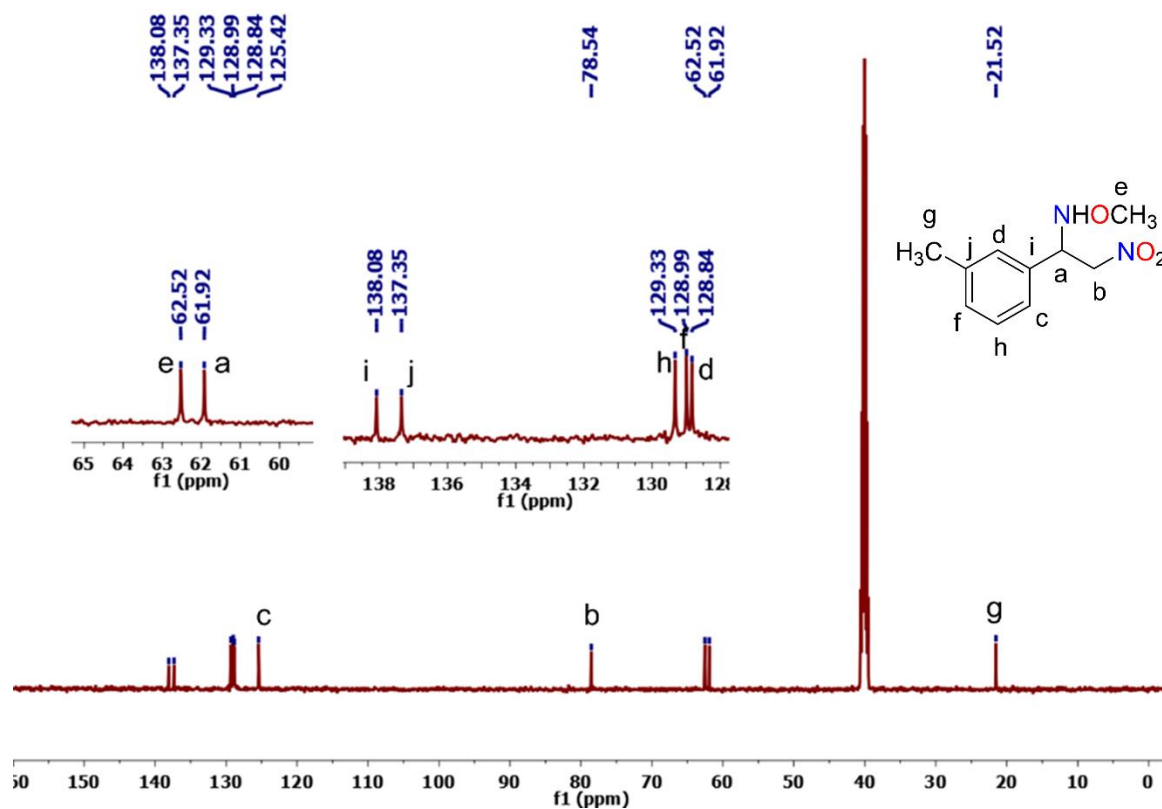
Figure S30: GC-MS spectra of N-(1-(4-fluorophenyl)-2-nitroethyl)-O-methylhydroxylamine (2d) in CH$_3$OH.
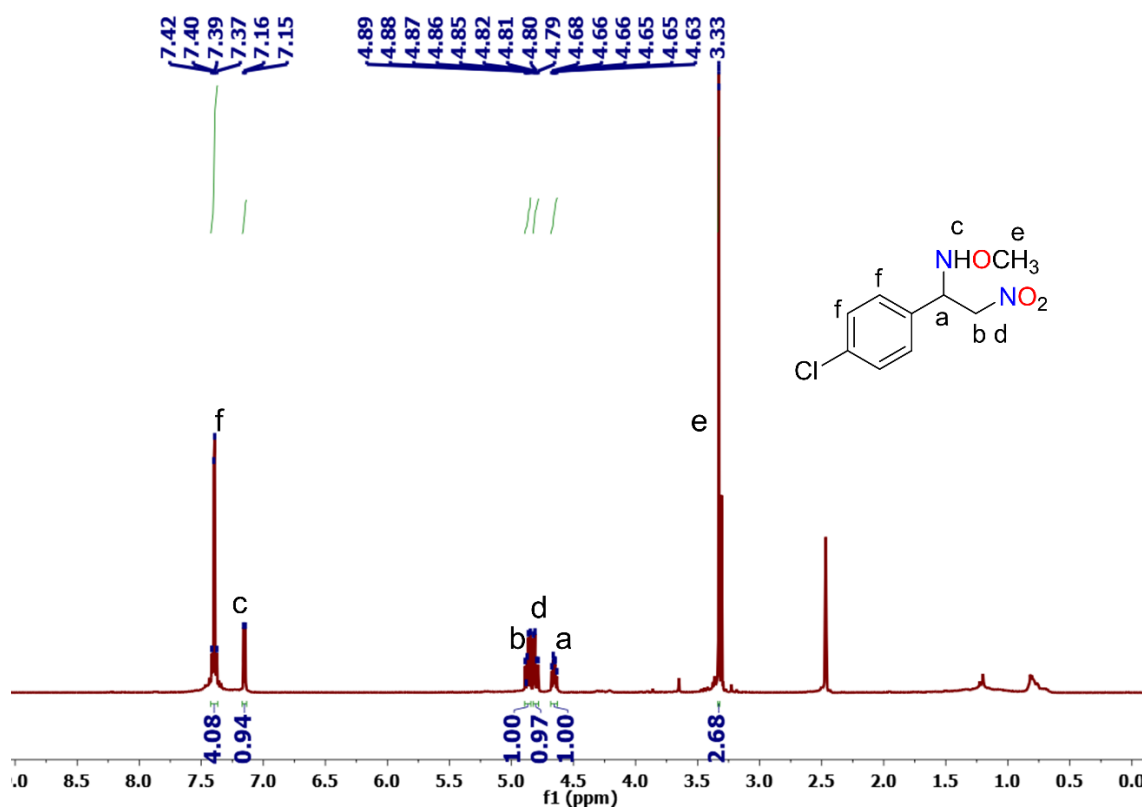
Figure S31: ^{1}H NMR spectra of N-(1-(4-chlorophenyl)-2-nitroethyl)-O-methylhydroxylamine (2e) in DMSO-d_6 using Bruker Avance DRX 400 (400 MHz) spectrometer.
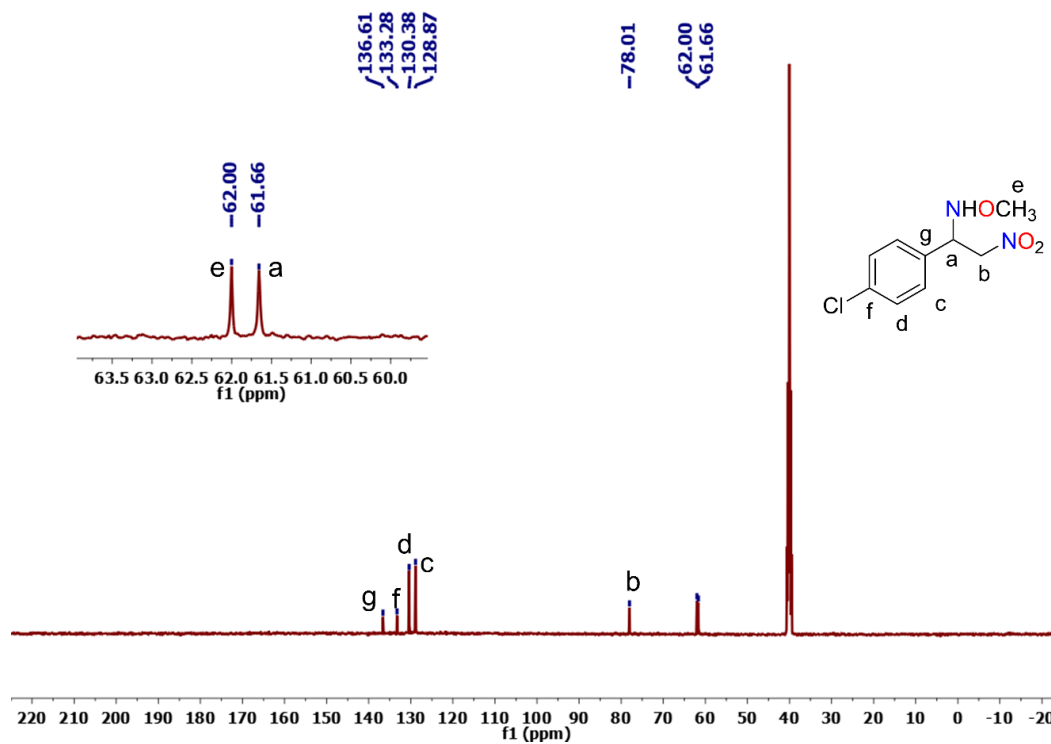
Figure S32: ^{13}C NMR spectra of N-(1-(4-chlorophenyl)-2-nitroethyl)-O-methylhydroxylamine (2e) in DMSO-d_6 using Bruker Avance DRX 400 (100 MHz) spectrometer.

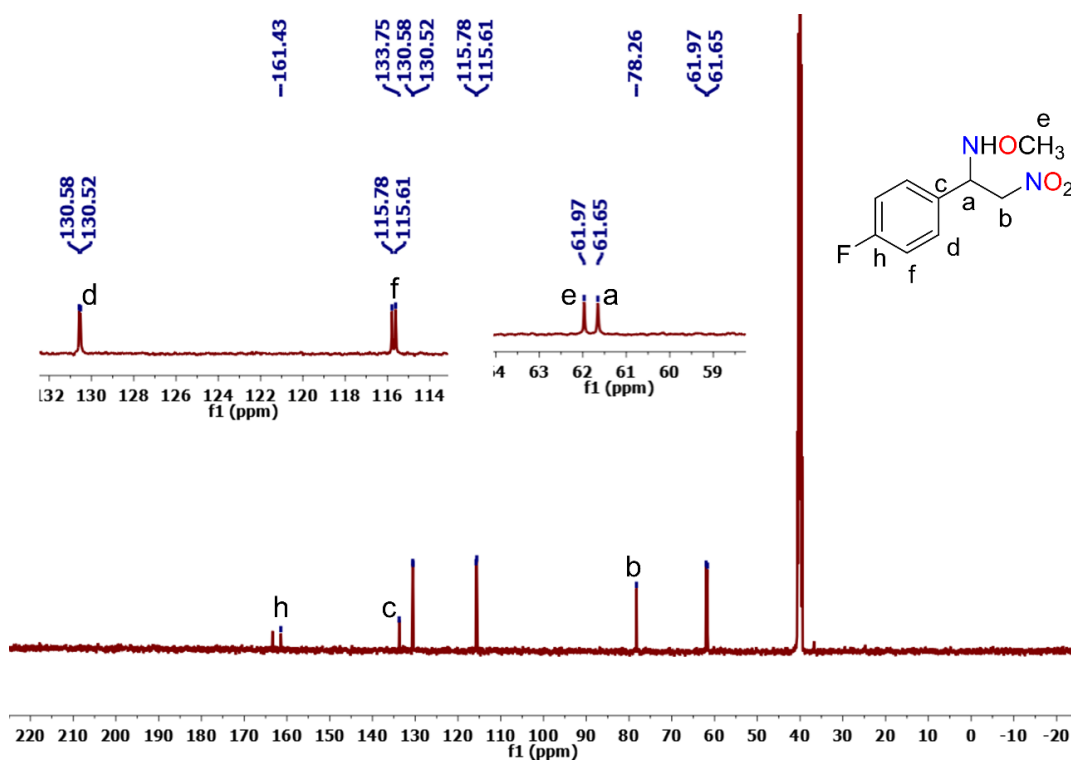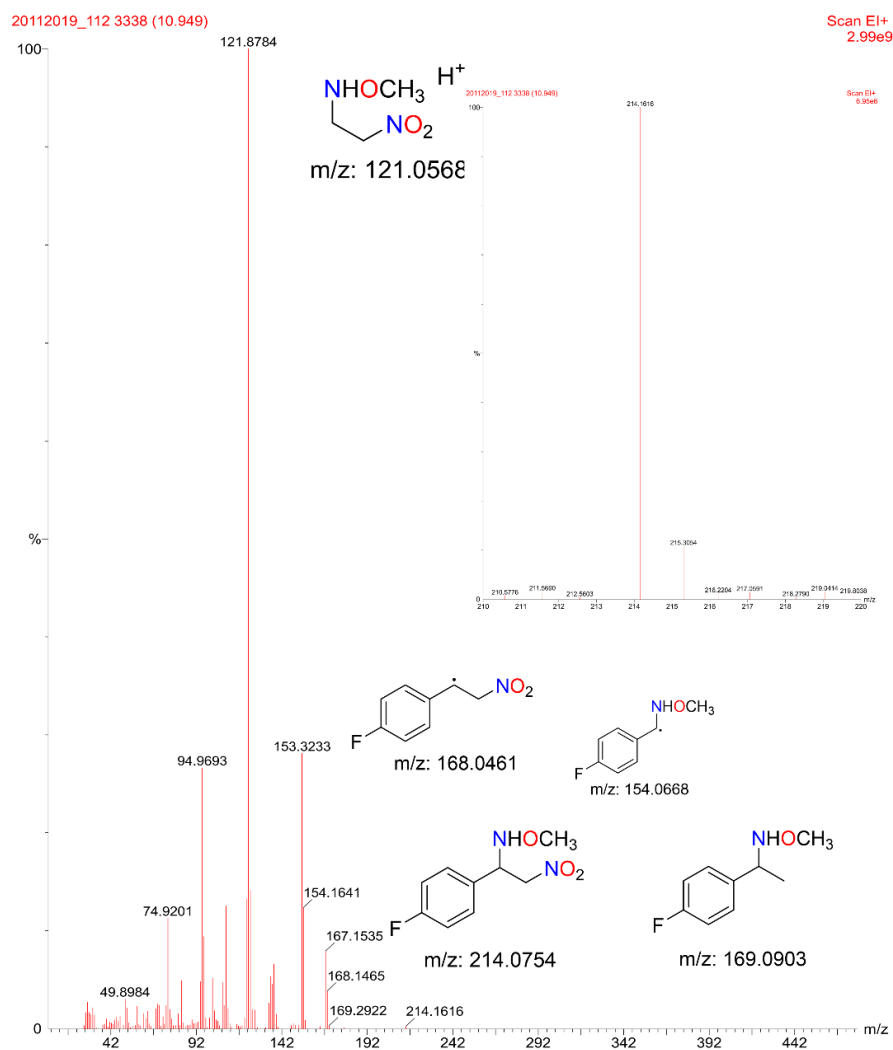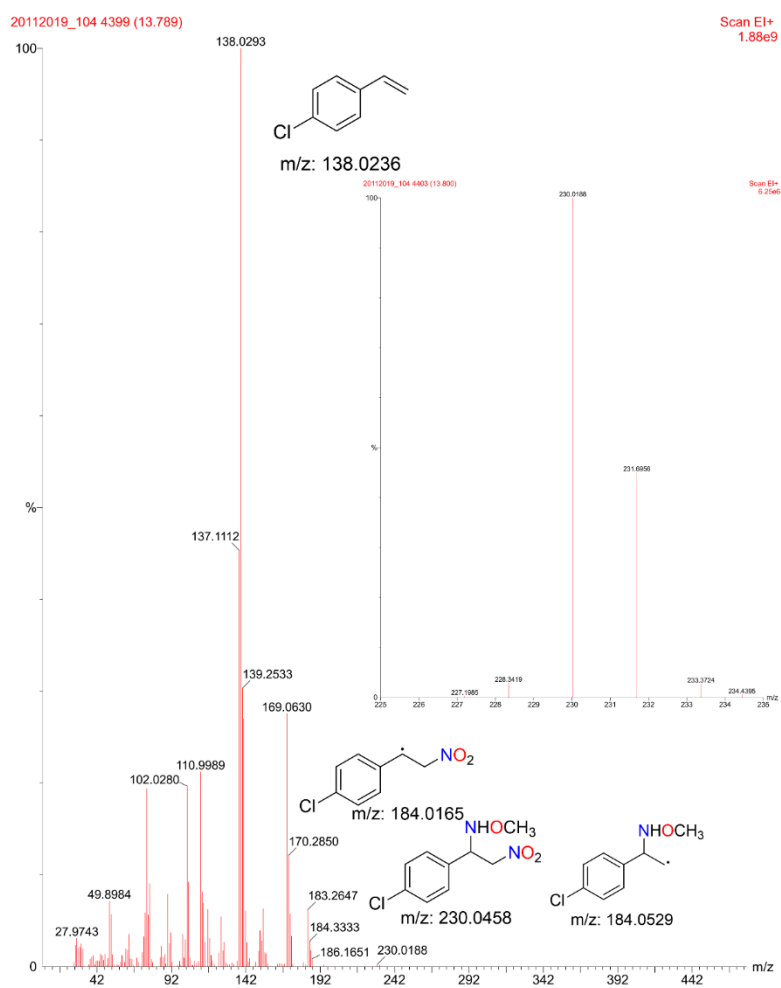**Figure S33:** GC-MS spectra of N-(1-(4-chlorophenyl)-2-nitroethyl)-O-methylhydroxylamine (2e) in CH₃OH.
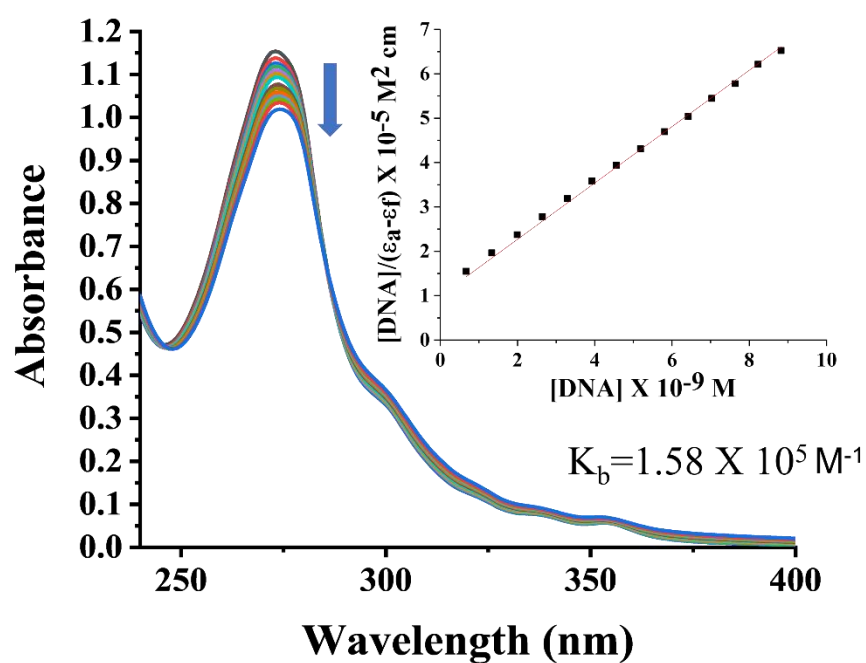
Figure S34: Absorption Spectral traces showing the decrease in the absorption intensity on gradual addition st-DNA (230μM) in aliquots to the solution of $[Pd(phen)(O_2CCH_3)_2]$ (25 µM) in MOPS buffer (pH 6.8) at 25°C having with the inset showing $[DNA]/(\varepsilon_a - \varepsilon_f) \times 10^{-5}$ M^2vs. $[DNA] \times 10^{-9}$ M^{-1} plot.

Equation	y = a + b*x		
Plot	Book1_B	Book1_C	Book1_D
Weight	No Weighting		
Intercept	1.00337 ± 0.0051	1.01081 ± 0.0049	0.99817 ± 0.0051
Slope	2.51443 ± 0.0707	0.81056 ± 0.0684	3.68486 ± 0.0704
Residual Sum of Square	4.87953E-4	4.5698E-4	4.83838E-4
Pearson's r	0.99724	0.97593	0.99872
R-Square (COD)	0.99449	0.95244	0.99745
Adj. R-Square	0.9937	0.94565	0.99708
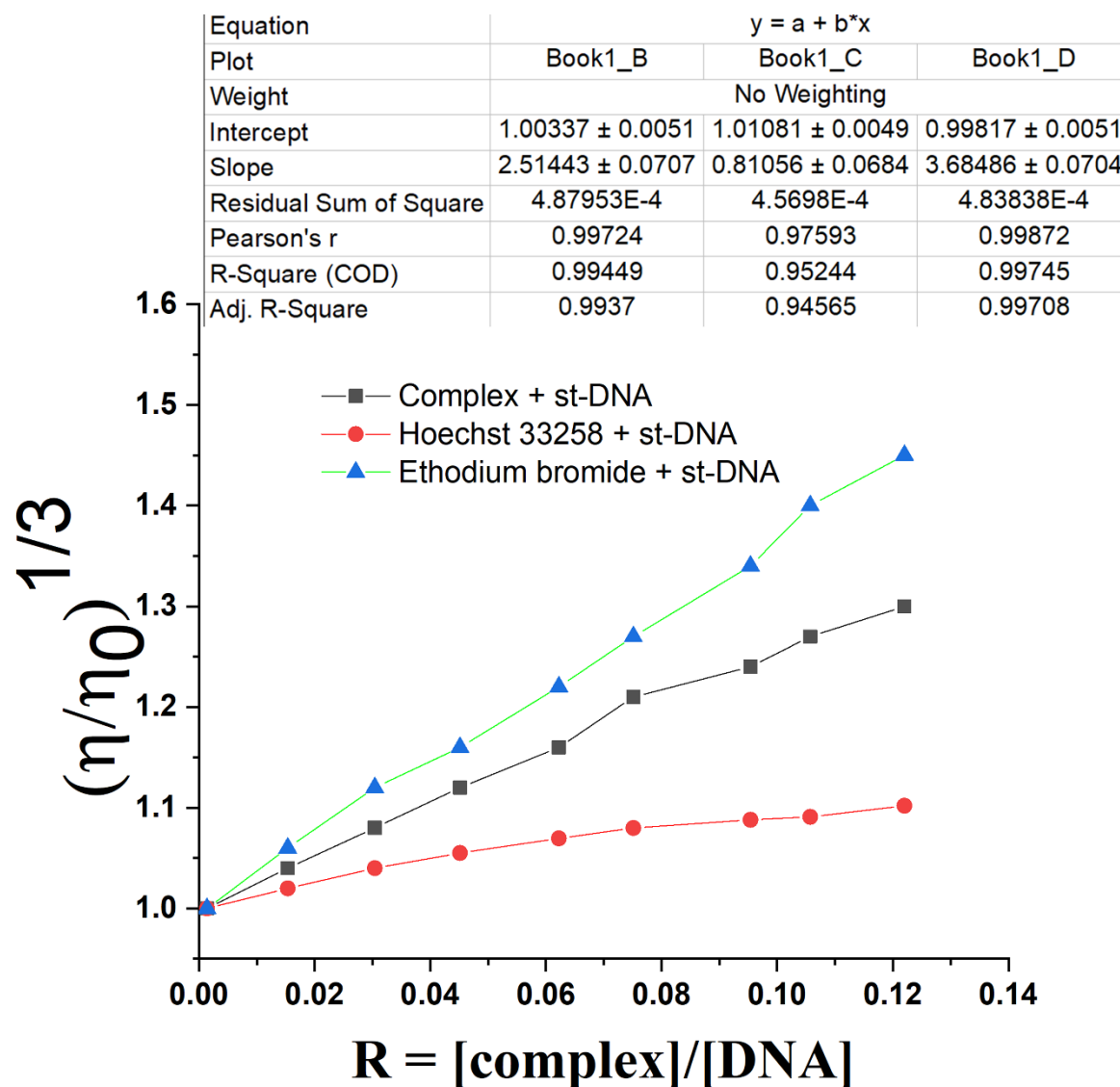
Figure S35: The effect of addition of increasing amount of pd complex, Ethidium Bromide and Hoechst 33258 on the relative viscosity of st-DNA at 25.0 ($\pm$ 0.1) °C in 5 mM Tris-HCl buffer (pH 7.2) ([DNA] = 0.5 mM, [complex] = 0 – 100 μM).

No.	Ret.Time min	Peak Name	Height mAU	Area mAU*min	Rel.Area %	Amount	Type
1	6.04	n.a.	397.893	379.473	100.00	n.a.	BMB
Total:			397.893	379.473	100.00	0.000	

Figure S36: HPLC chromatogram of O-methyl-N-(2-nitro-1-phenylethyl)hydroxylamine in presence of st-DNA in C18 column.

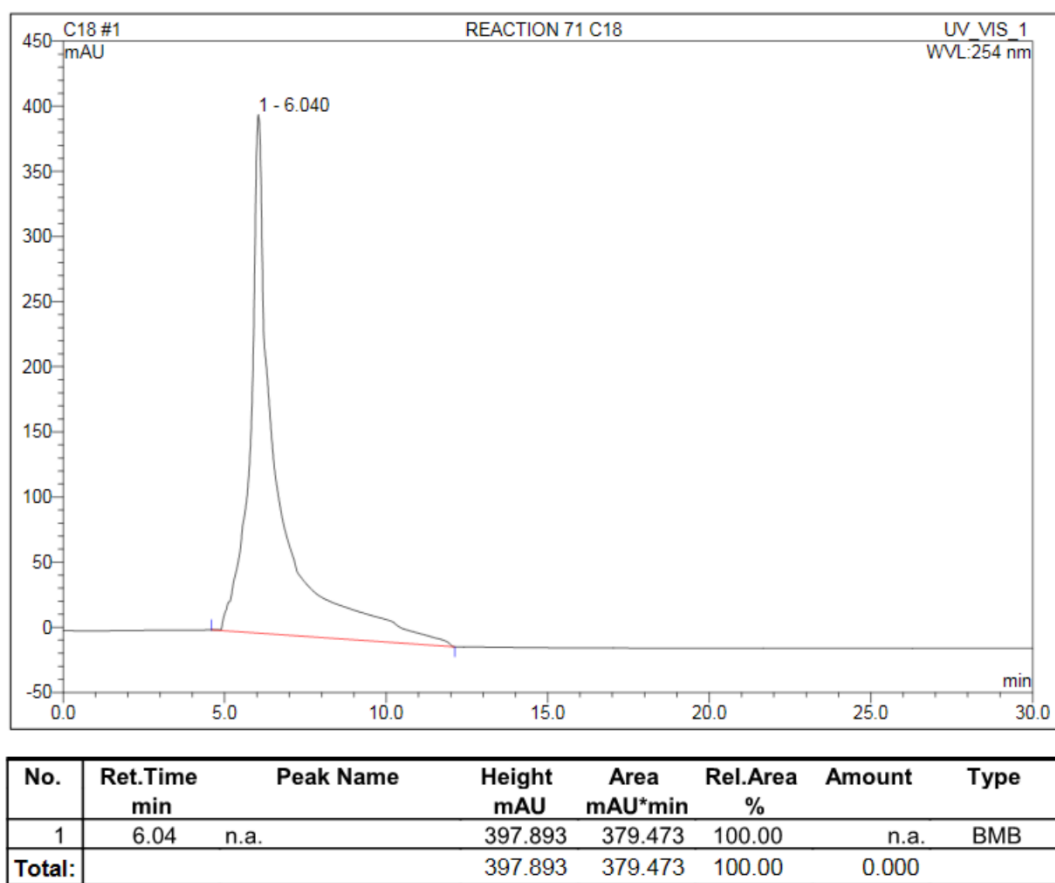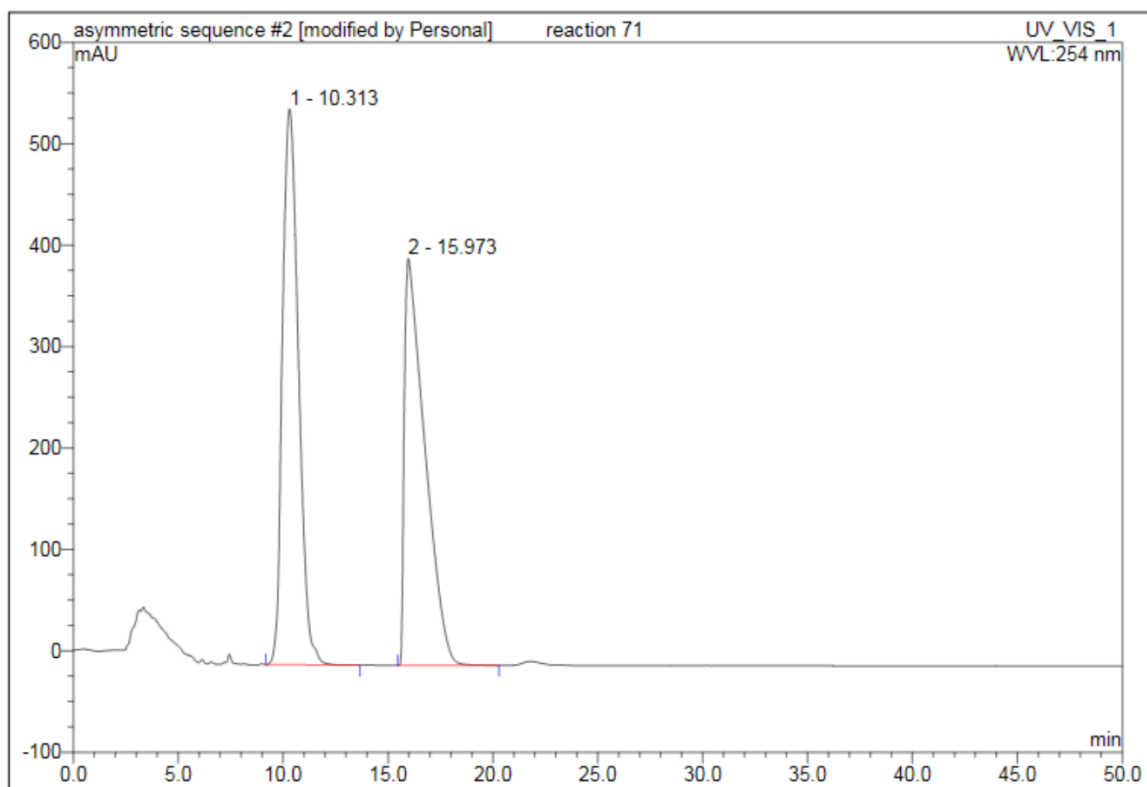| No.	Ret.Time min	Peak Name	Height mAU	Area mAU*min	Rel.Area %	Amount	Type
1	10.31	n.a.	548.058	485.330	51.74	n.a.	BMB*
2	15.97	n.a.	401.499	452.727	48.26	n.a.	BMB
Total:			949.557	938.057	100.00	0.000	

Figure S37: HPLC chromatogram of O-methyl-N-(2-nitro-1-phenylethyl)hydroxylamine (2a) without st-DNA in Chiralcel-ODH column.
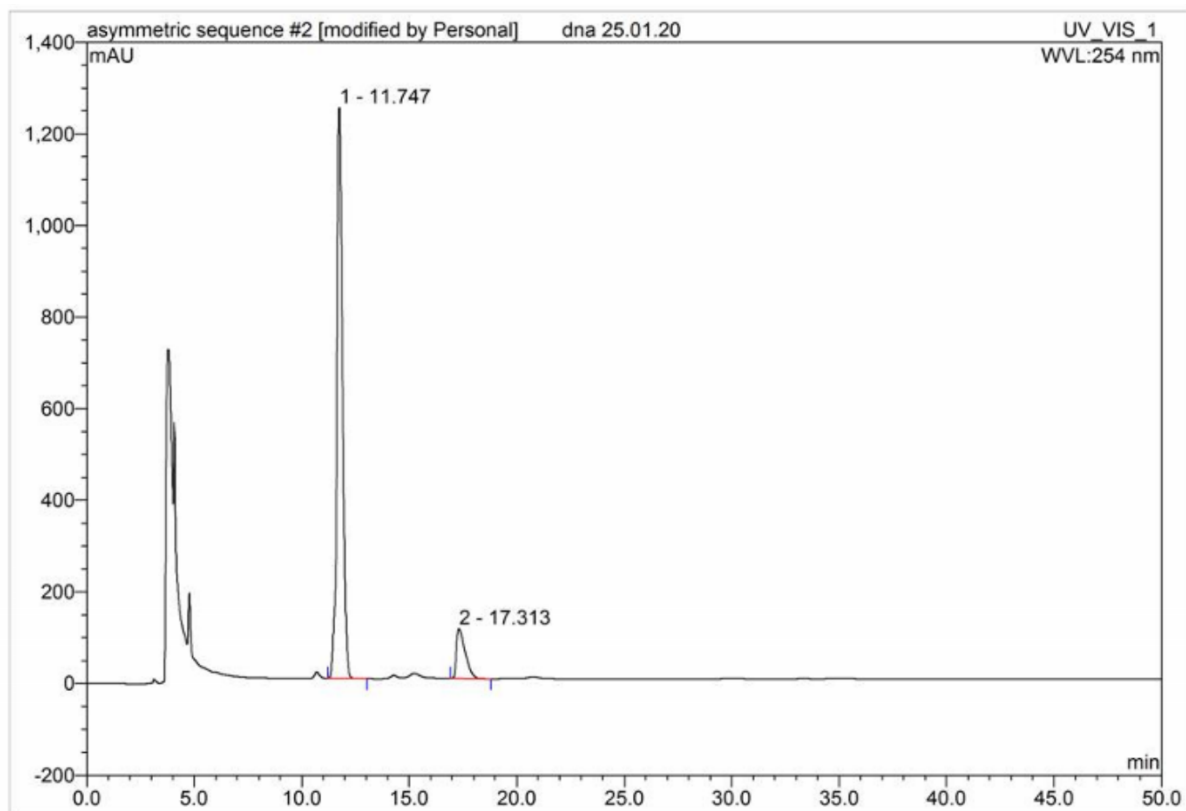
No.	Ret.Time min	Peak Name	Height mAU	Area mAU*min	Rel.Area %	Amount	Type
1	11.75	n.a.	1245.330	370.608	87.87	n.a.	BMB*
2	17.31	n.a.	108.033	51.160	12.13	n.a.	BMB*
Total:			1353.363	421.768	100.00	0.000	

Figure S38: HPLC chromatogram of O-methyl-N-(2-nitro-1-phenylethyl)hydroxylamine (3a) in presence of st-DNA in Chiralcel-ODH column.
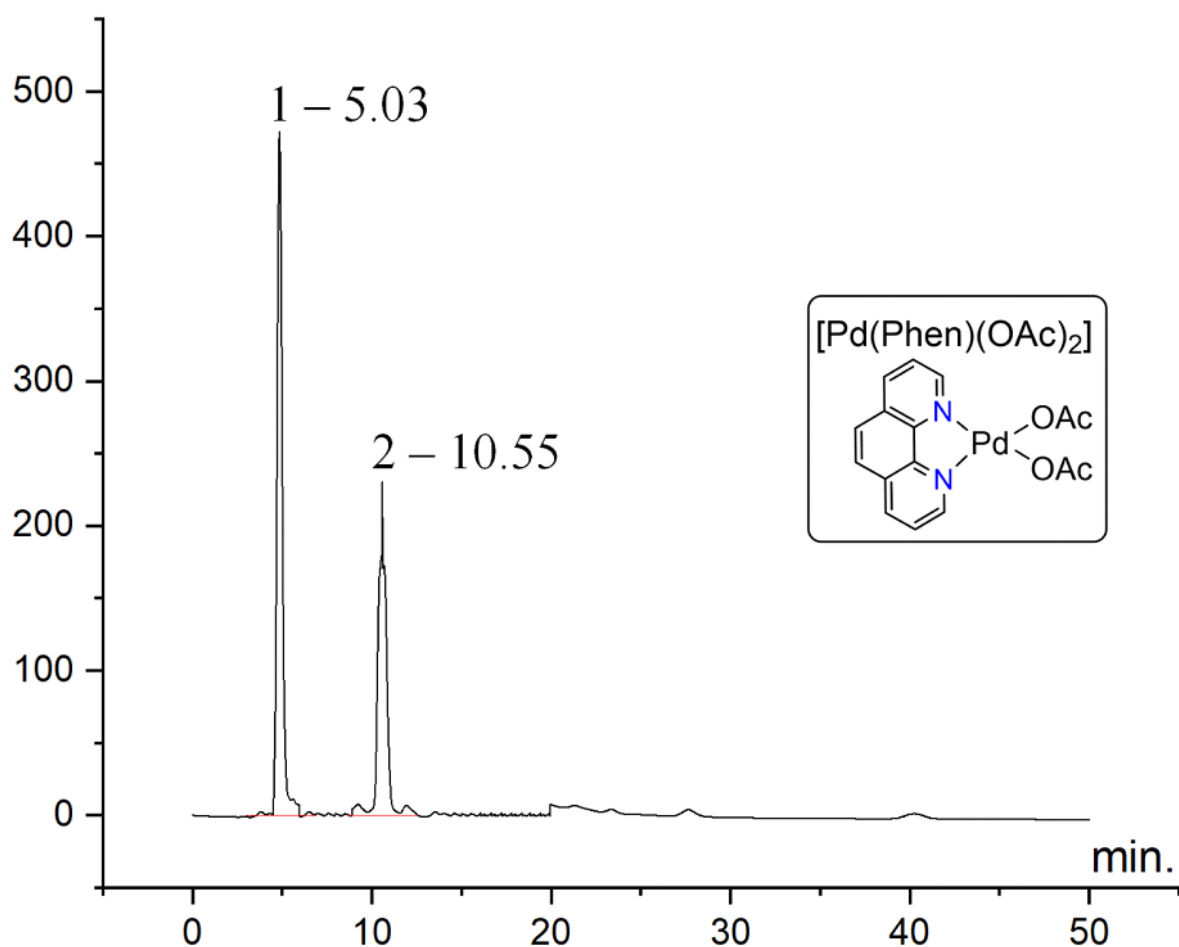
No.	Ret. Time min	Peak Name	Hight mAU	Rel.Area %	Amount	Type
1	5.03	n.a	462.392	62.34	n.a	BMB*
2	10.55	n.a	242.342	38.66	n.a	BMB
Total:				100		

Figure S39: HPLC chromatogram of N-(1-(4-methoxyphenyl)-2-nitroethyl)-O-methylhydroxylamine (3b) without st-DNA in Chiralcel-ODH column.

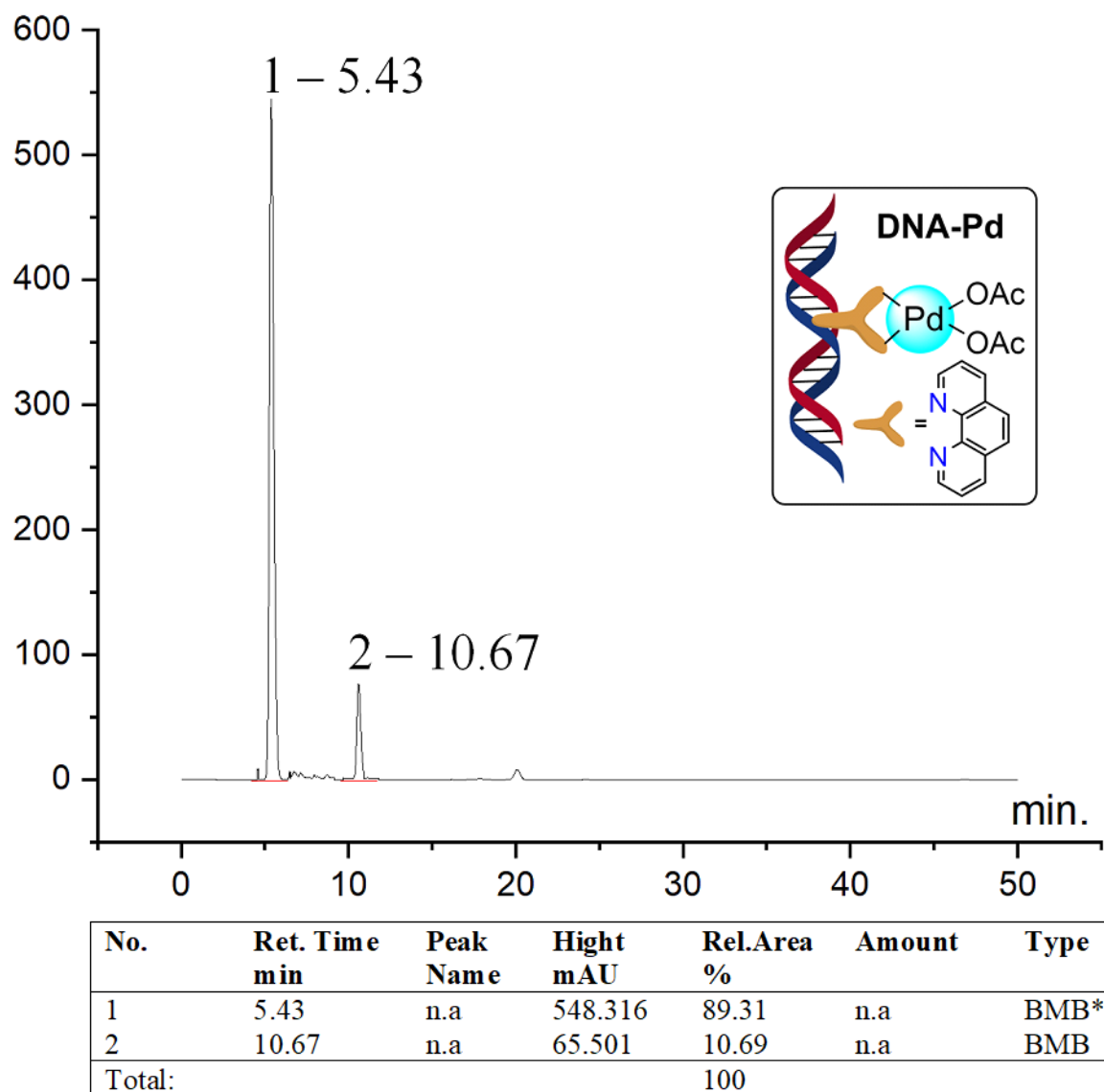| No.	Ret. Time min	Peak Name	Hight mAU	Rel.Area %	Amount	Type
1	5.43	n.a	548.316	89.31	n.a	BMB*
2	10.67	n.a	65.501	10.69	n.a	BMB
Total:				100		

Figure S40: HPLC chromatogram of N-(1-(4-methoxyphenyl)-2-nitroethyl)-O-methylhydroxylamine (3b) in presence of st-DNA in Chiralcel-ODH column.
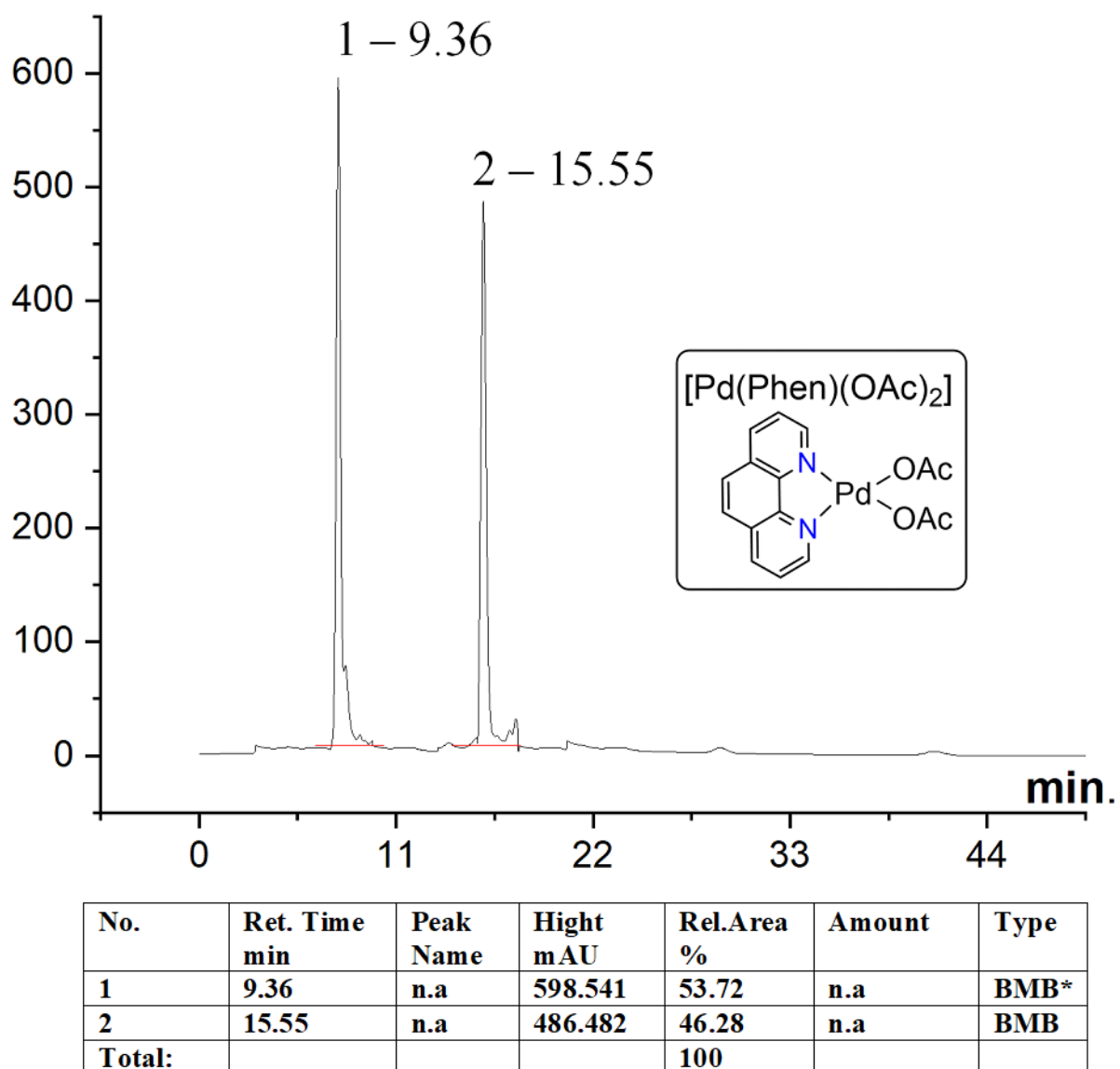
No.	Ret. Time min	Peak Name	Hight mAU	Rel.Area %	Amount	Type
1	9.36	n.a	598.541	53.72	n.a	BMB*
2	15.55	n.a	486.482	46.28	n.a	BMB
Total:				100		

Figure S41: HPLC chromatogram of O-methyl-N-(2-nitro-1-(m-tolyl) ethyl) hydroxylamine (3c) without st-DNA in Chiralcel-ODH column.

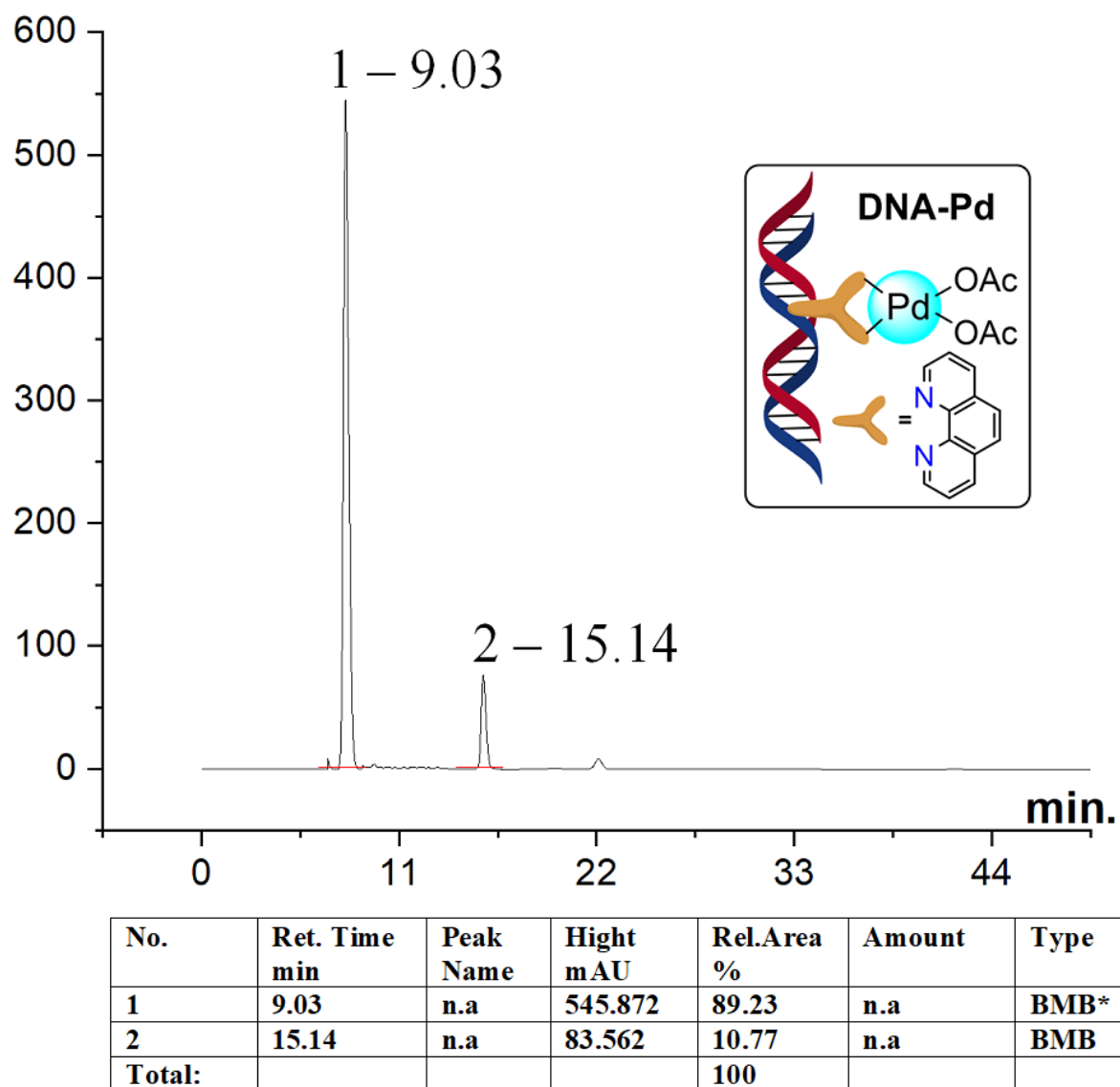| No.	Ret. Time min	Peak Name	Hight mAU	Rel.Area %	Amount	Type
1	9.03	n.a	545.872	89.23	n.a	BMB*
2	15.14	n.a	83.562	10.77	n.a	BMB
Total:				100		

Figure S42: HPLC chromatogram of O-methyl-N-(2-nitro-1-(m-tolyl) ethyl) hydroxylamine (3c) in presence of st-DNA in Chiralcel-ODH column.

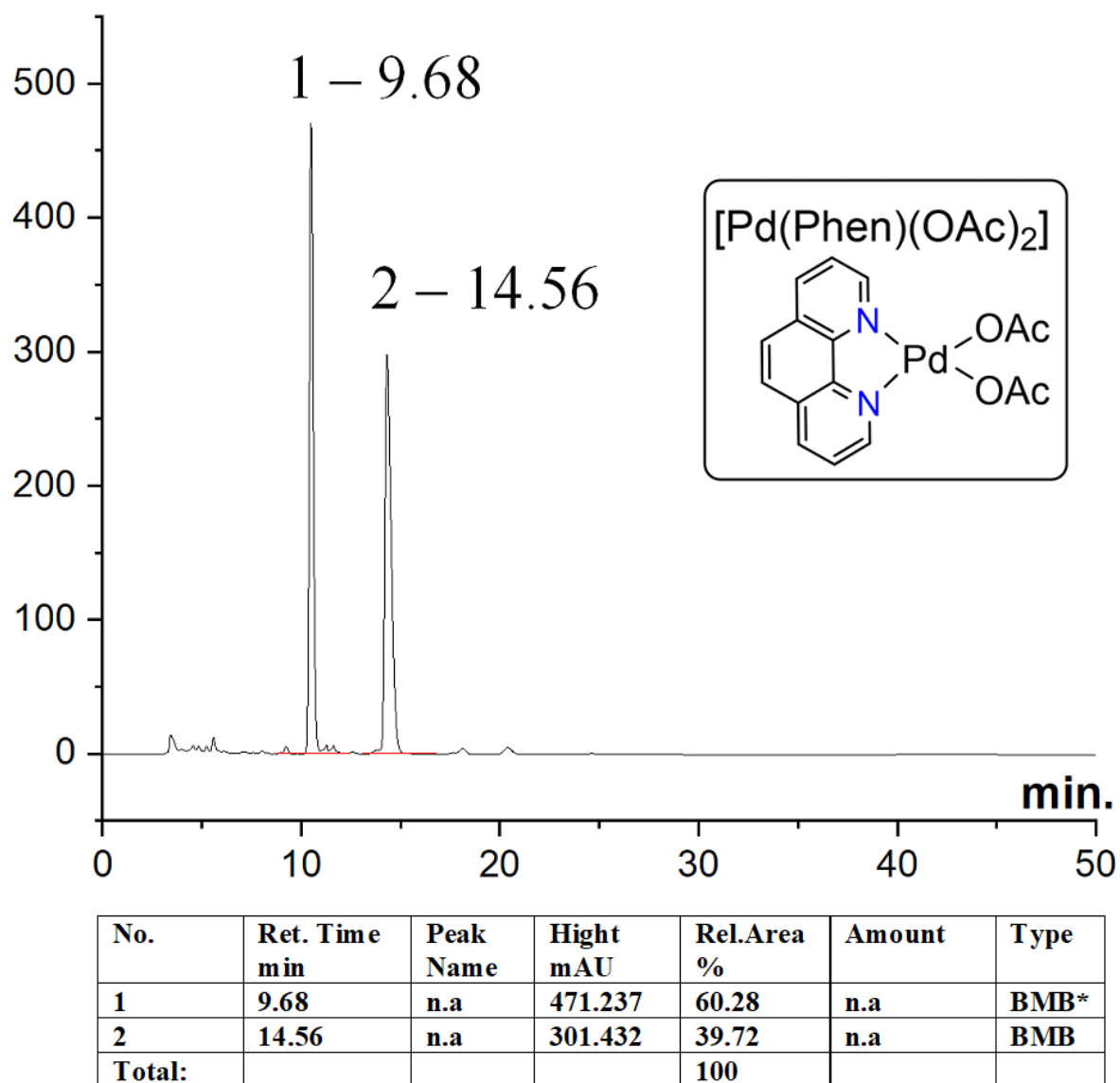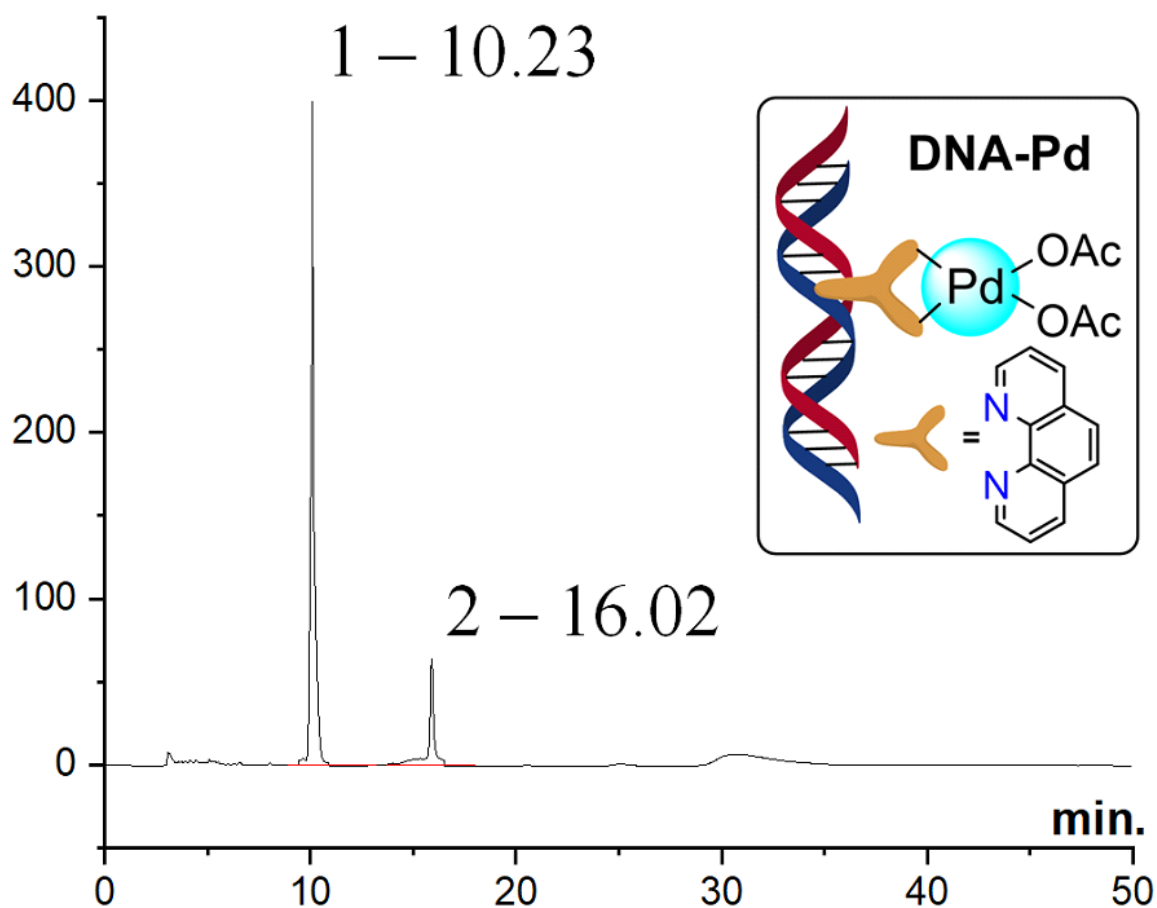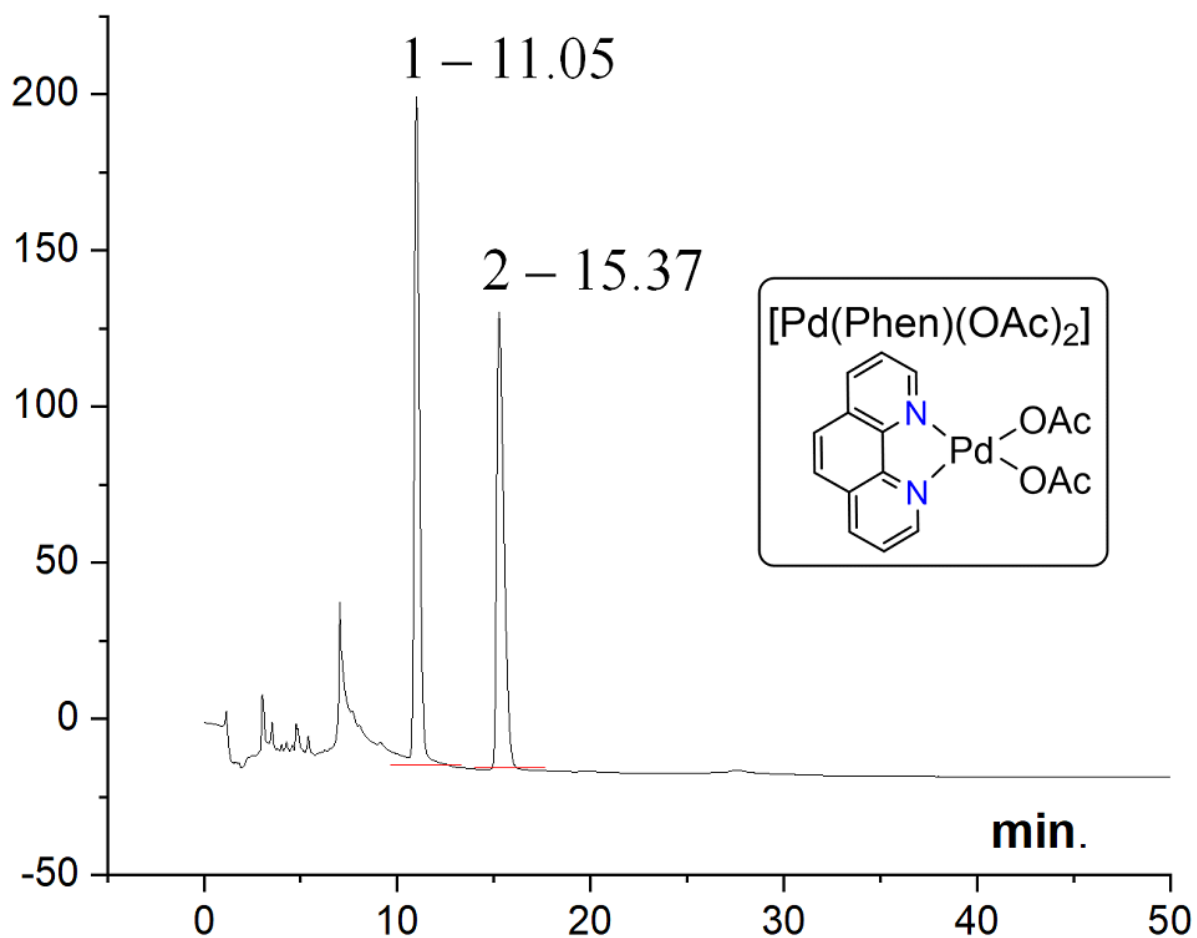| No.	Ret. Time min	Peak Name	Hight mAU	Rel.Area %	Amount	Type
1	9.68	n.a	471.237	60.28	n.a	BMB*
2	14.56	n.a	301.432	39.72	n.a	BMB
Total:				100		

Figure S43: HPLC chromatogram of N-(1-(4-fluorophenyl)-2-nitroethyl)-O-methylhydroxylamine (3d) without st-DNA in Chiralcel-ODH column.

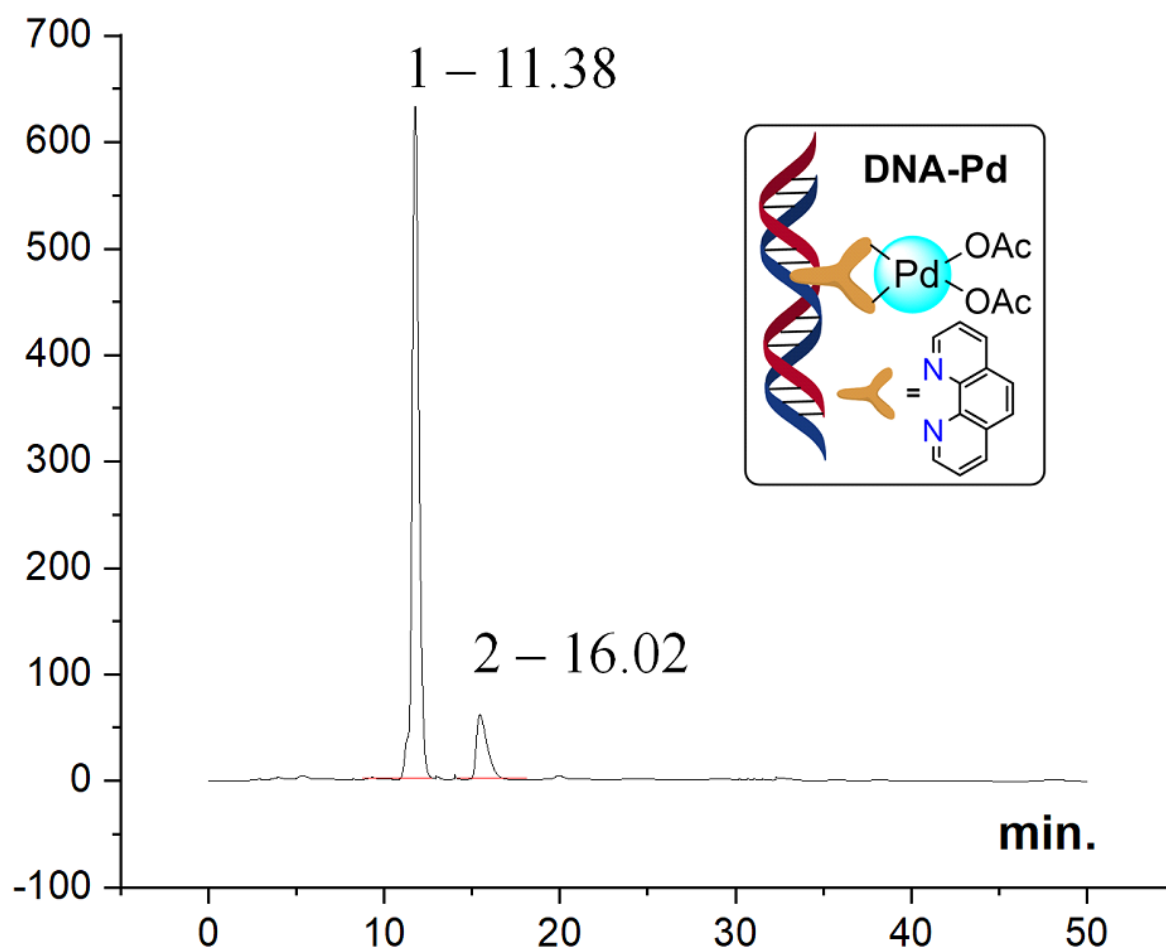| No.	Ret. Time min	Peak Name	Hight mAU	Rel.Area %	Amount	Type
1	10.23	n.a	402.473	91.54	n.a	BMB*
2	16.02	n.a	69.47	8.46	n.a	BMB
Total:				100		

Figure S44: HPLC chromatogram of N-(1-(4-fluorophenyl)-2-nitroethyl)-O-methylhydroxylamine (3d) in presence of st-DNA in Chiralcel-ODH column.

No.	Ret. Time min	Peak Name	Hight mAU	Rel.Area %	Amount	Type
1	11.05	n.a	204.529	54.36	n.a	BMB*
2	15.37	n.a	131.622	45.64	n.a	BMB
Total:				100		

Figure S45: HPLC chromatogram of N-(1-(4-chlorophenyl)-2-nitroethyl)-O-methylhydroxylamine (3e) without st-DNA in Chiralcel-ODH column.

No.	Ret. Time min	Peak Name	Hight mAU	Rel.Area %	Amount	Type
1	11.38	n.a	634.350	94.35	n.a	BMB*
2	16.02	n.a	83.241	5.65	n.a	BMB
Total:				100		

Figure S46: HPLC chromatogram of N-(1-(4-chlorophenyl)-2-nitroethyl)-O-methylhydroxylamine (3e) in presence of st-DNA in Chiralcel-ODH column.
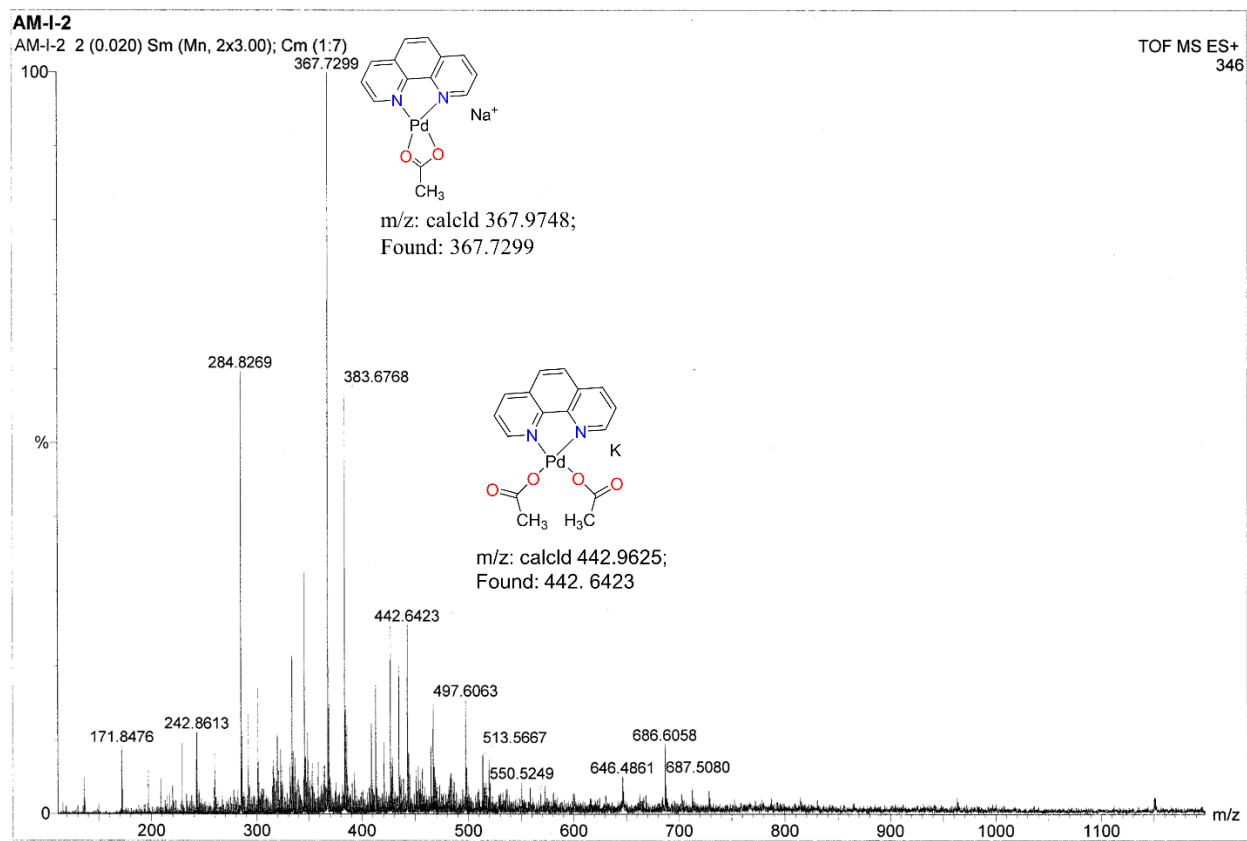
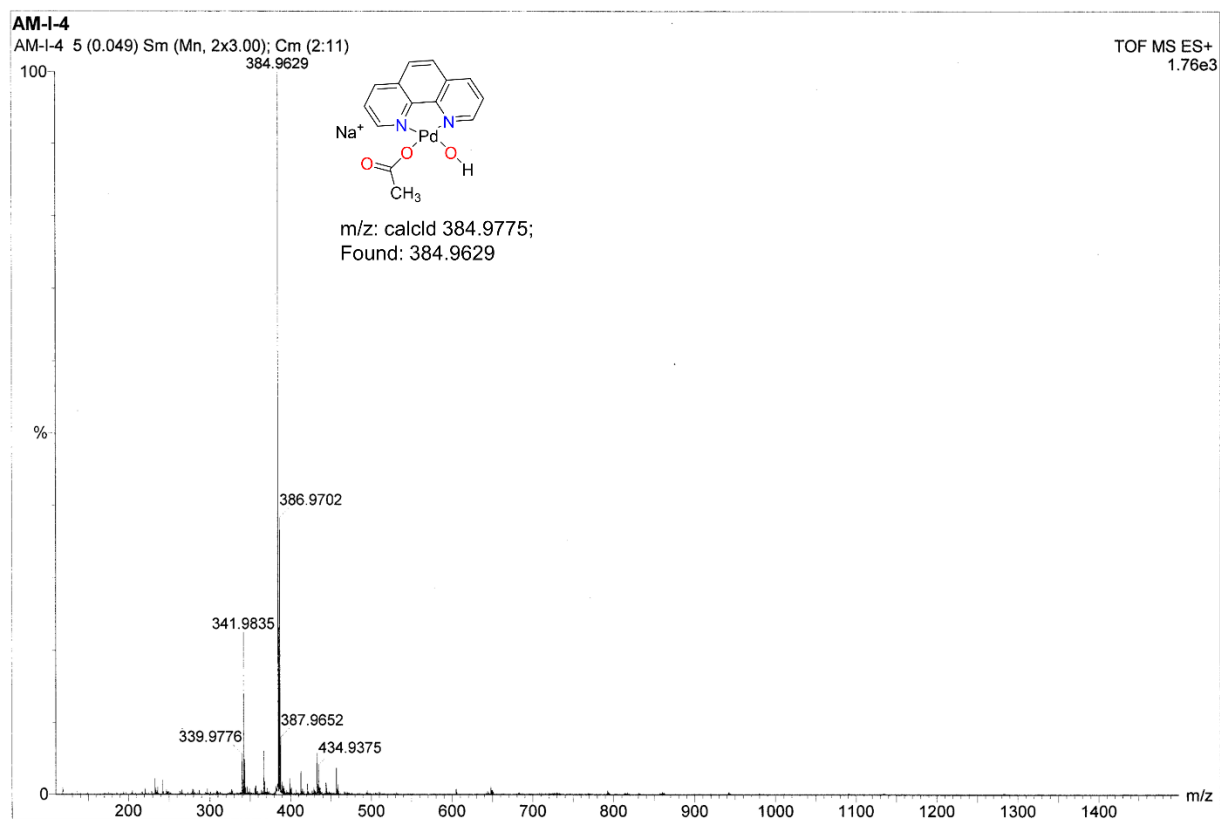**Figure S47**: HRMS spectra of the reaction mixture after completing 4 hrs in CH$_3$OH.

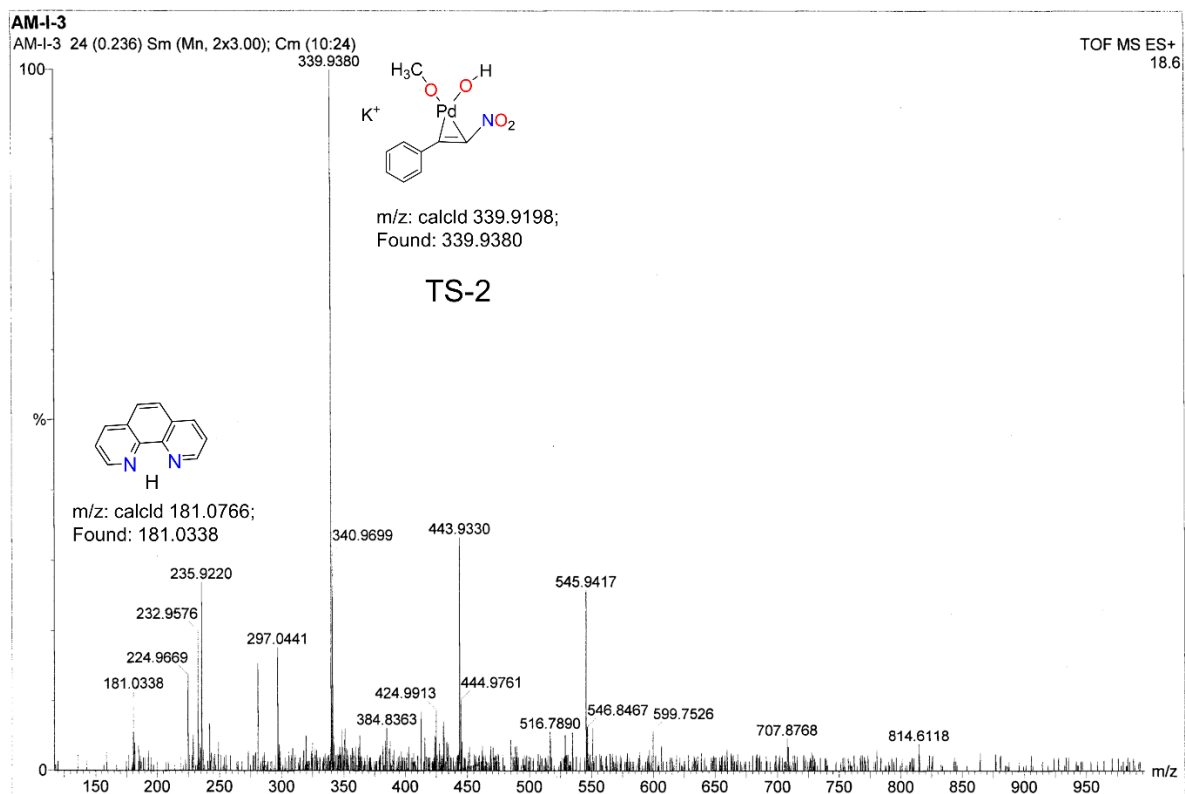**Figure S48:** HRMS spectra of the reaction mixture after completing 8 hrs in CH$_3$OH.

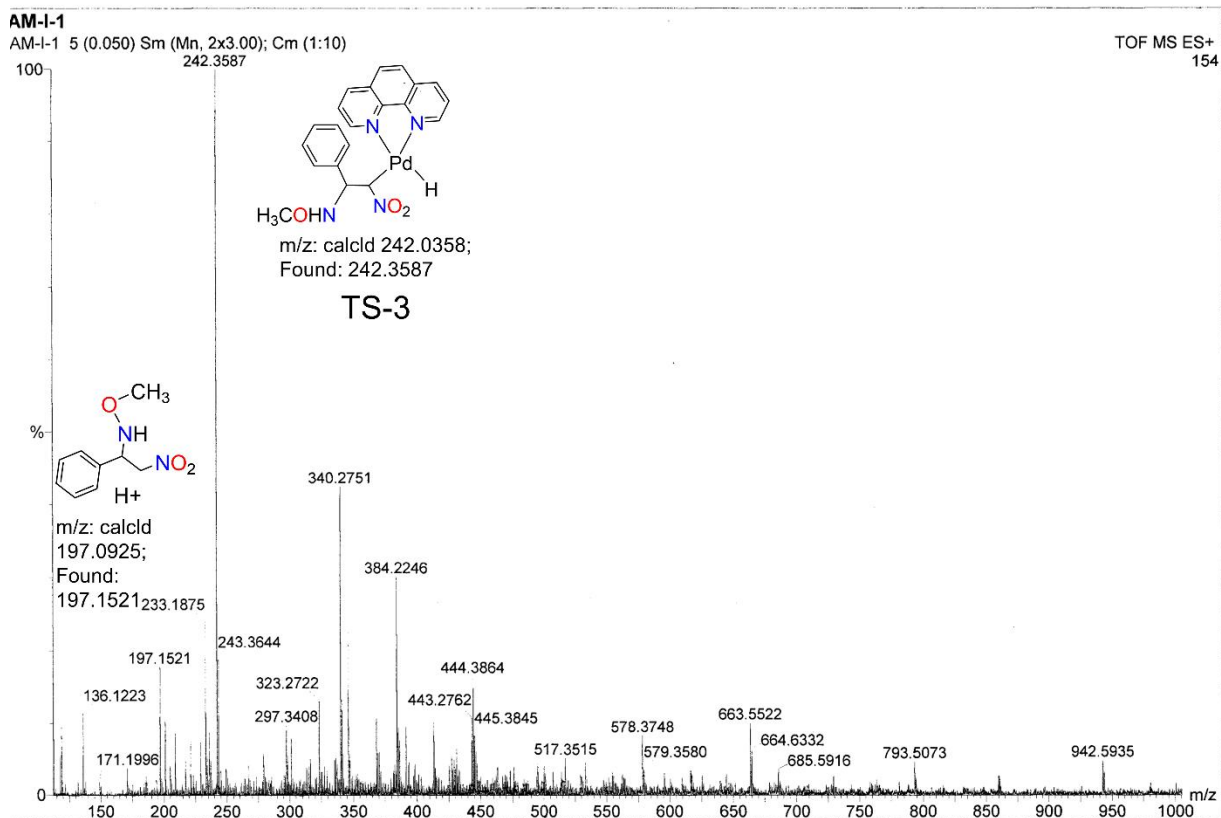**Figure S49:** HRMS spectra of the reaction mixture after completing 12 hrs in CH$_3$OH.

Figure S50: HRMS spectra of the reaction mixture after completing 16 hrs in CH$_3$OH.
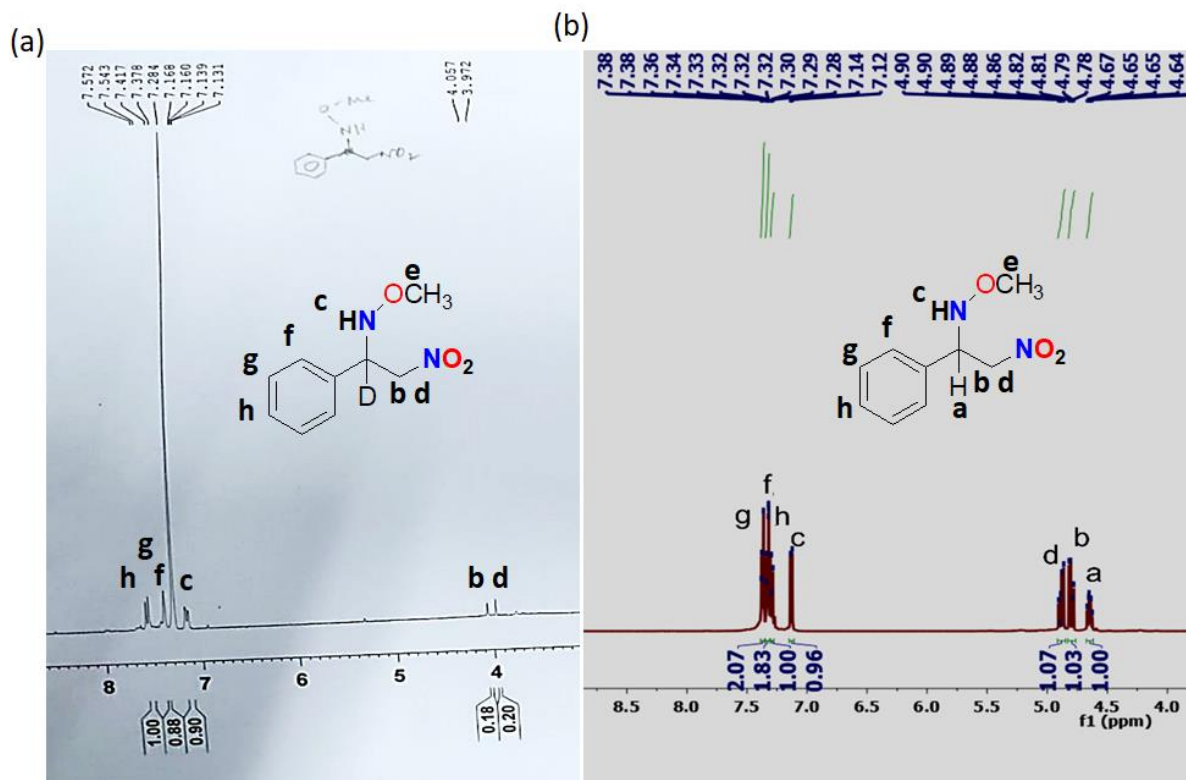
Figure S51: (a) Proposed catalytic cycle of Pd-catalysed hydroamination reaction with deuterated buffer medium; **(b)** Proposed catalytic cycle of Pd-catalysed hydroamination reaction with MOPS buffer medium.
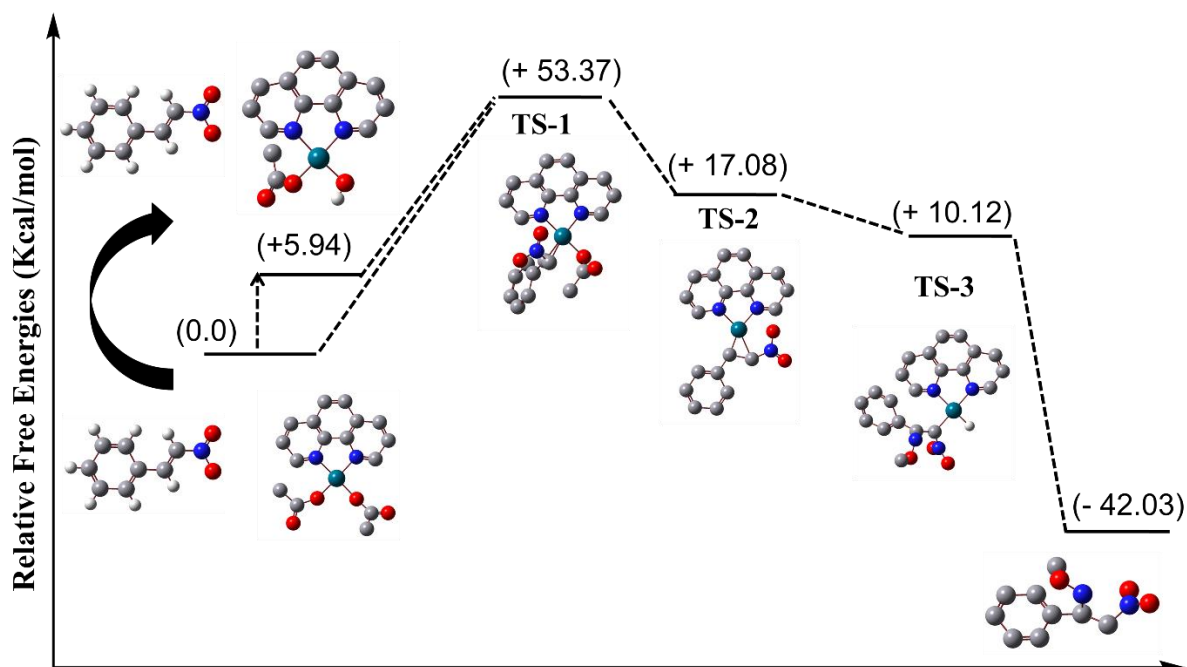

Figure S52: DFT study of the reaction mechanism of the palladium catalyst with β-nitrostyrene. All data (in Kcal/mol) have been calculated B3LYP/6-31G(d,p)/LanL2DZ level.
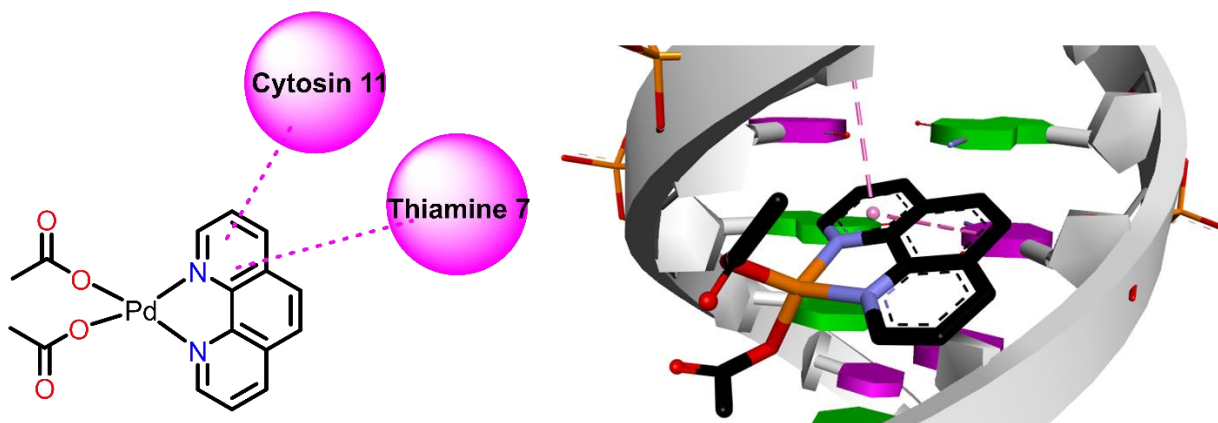

Figure S53: Docked pose and interactions of [(phen)Pd(O$_2$CCH$_3$)$_2$] complex in the DNA minor grove by intercalation.
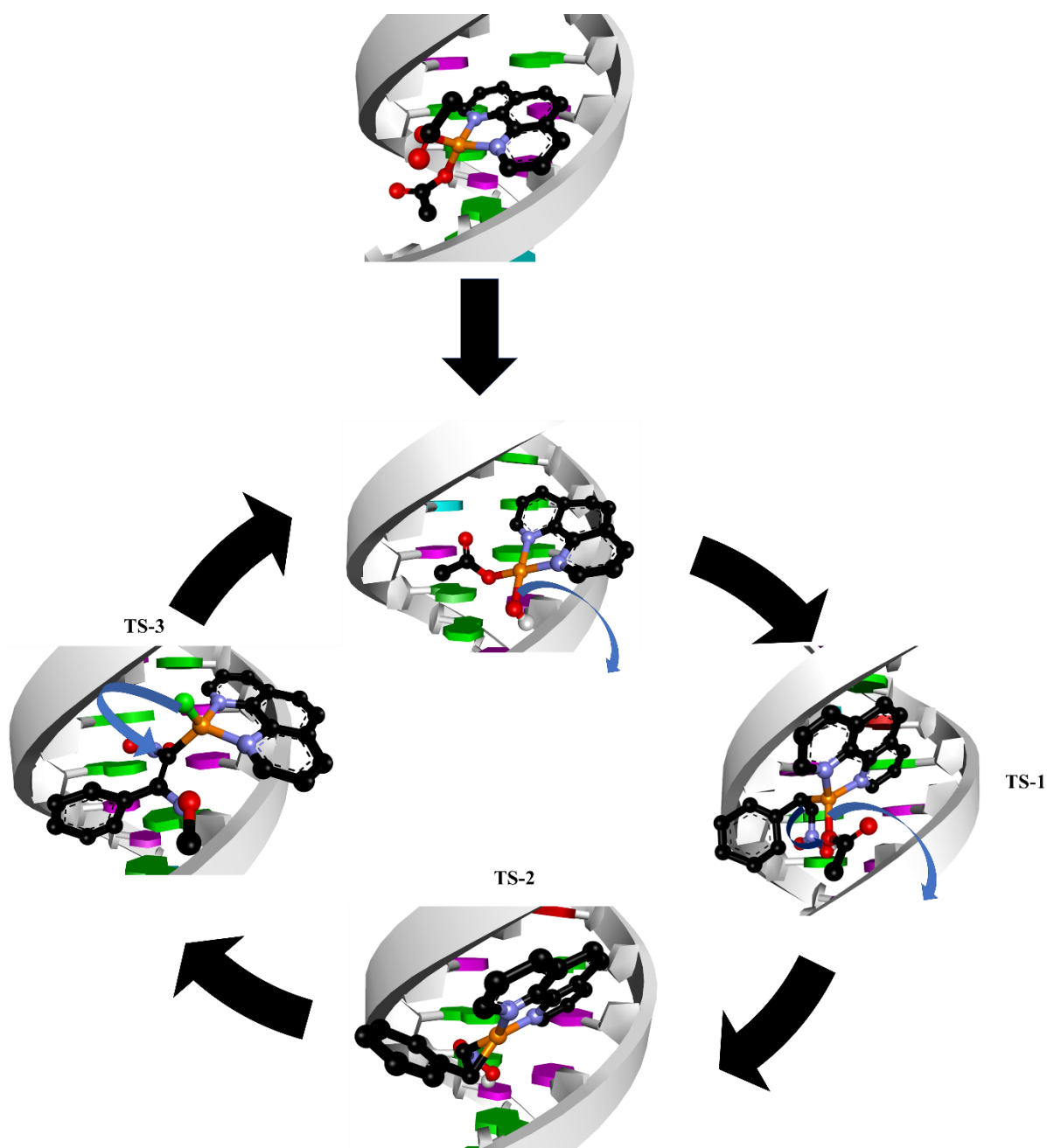
Figure S54: Mechanism of the formation of R isomer by the complex intercalated DNA by molecular docking studies. (The docking was performed in DNA with grid box 60 X 70 X 120 Å grid points and 0.375 Å spacing. Prior to molecular docking water molecules were removed, polar hydrogens were added and Gestiger charges were added to the DNA. The parameters for Pd were included in the software and other forcefields were restrained during the calculations).